Hybrid Nanofluid flow with Modified Fourier Law in a Rotating frame

Thesis Submitted By

Noor Us Saba

(01-248192-005)

Supervised By

Prof. Dr. M. Ramzan

A dissertation submitted to the Department of Computer Science, Bahria University Islamabad as a partial fulfillment of the requirements for the award of the degree of MS (Mathematics)

Session (2019-2021)

Bahria University
Discovering Knowledge

MS-13

THESIS COMPLETION CERTIFICATE

Student's Name: **Noor Us Saba** Registration No. **63119** Programme of Study: **MS MATHEMATICS**

Thesis Title: **Hybrid Nanofluid flow with modified Fourier Law in a rotating frame**

It is to certify that the above student's thesis has been completed to my satisfaction and, to my belief, its standard is appropriate for submission for Evaluation. I have also conducted plagiarism test of this thesis using HEC prescribed software and found similarity index at 2% that is within the permissible limit set by the HEC for the MS/MPhil degree thesis. I have also found the thesis in a format recognized by the BU for the MS/MPhil thesis.

Principal Supervisor's Signature: _____

Date: ___15-10-2021_____ Name: __Prof._Dr. Muhammad Ramzan_

Bahria University
Discovering Knowledge

MS-14A

Author's Declaration

I Noor Us Saba, hereby state that my MS thesis titled "Hybrid Nanofluid flow with Modified Fourier Law in a Rotating frame" is my own work and has not been submit previously by me for taking any degree from university Bahria University or anywhere else in the country/world.

At any time if my statement is found to be incorrect even after my graduate the university has the right to withdraw/ cancel my MS degree.

Name of student: Noor Us Saba

Date: 15-10-2021

Bahria University
Discovering Knowledge

MS-14B

Plagiarism Undertaking

I, solemnly declare that research work presented in thesis titled "Hybrid Nanofluid flow with Modified Fourier Law in a Rotating frame" is solely my research work with no significant contribution from any other person. Small contribution/ help wherever taken has been duly acknowledged and that complete thesis has been written by me.

I understand the zero tolerance policy of the HEC and Bahria University towards plagiarism. Therefore, I as an Author of above titled declare that no portion of my thesis has been plagiarized and any material used as references is properly referred/cited.

I understand that if I am found guilty of any formal plagiarism in the above titled thesis even after award of MS degree, the university reserved the right to withdraw/revoke my MS degree and that HEC and the University has the right to publish my name on the HEC/University website on which names of students are placed who submitted plagiarized thesis.

I have also conducted plagiarism test of this thesis using HEC prescribed software and found similarity index at 1% that is within the permissible limit set by the HEC for the MS/MPhil degree thesis

Student/ Author's Sign:

Name of the Student: Noor Us Saba

Dedicated to my exceptional parents and teachers whose tremendous support and cooperation led me to this wonderful accomplishment

Acknowledgments

I am thankful to Almighty ALLAH Who has enabled me to learn and to achieve milestones towards my destination and His beloved Prophet Hazrat Muhammad (ﷺ) Who is forever a constant source of guidance, a source of knowledge and blessing for entire creation. His teachings show us a way to live with dignity, stand with honor and learn to be humble.

My acknowledgment is to my kind, diligent and highly zealous supervisor, Prof. Dr. M. Ramzan, who supported me with his cherished opinions and inspirational discussions. His valuable expertise, comments, suggestions and instructions are most welcome that greatly improved the clarity of this document. I am placing my earnest thanks to Prof. Dr. M. Ramzan. I am so grateful to work under the supervision of such a great person.

My gratitude is to my honorable professors who took me to the apex of my academia with their guidance. In particular, Prof. Dr. Rizwan and Dr. Jafar Hasnain who have always been supportive in all of my course work and kept encouraging me throughout the session in Bahria University, Islamabad Campus. They are the true teachers who have made Mathematics Department of BUIC, a real place of learning.

My intense recognition is to my parents and my adored siblings (for everything) who are always real pillars for my encouragement and showered their everlasting love, care and support throughout my life. Humble prayers, continuing support and encouragement of my family are as always highly appreciated. I also appreciate the moral support of all my friends, Maryam and Maham, especially Nazia Shahmir and all PhD scholars who did cooperation up to his best and help me at every step and stage at my research work. Consequently, My all plea is to Allah, the Almighty, the beneficent Whose blessings are always showered upon me via strengthening my wis- dom and bestowed me with the knowledge of what he wants.

Noor Us Saba

Bahria University Islamabad, Pakistan

October, 2021

Abstract

This study aims to investigate time independent rotating frame of hybrid nanofluid flow-based ethylene glycol consisting of copper (Cu) and copper oxide (CuO) amidst two horizontal parallel plates. The upper plate is porous while lower one is stretching with a variable velocity. The suggested model is analysed with modified Fourier's law under the effect of thermal stratification. However, the impact of Coriolis force along with centripetal force is examined for the enhancement of mathematical model. Relevant similarity transformation method is supplemented for the conversion of partial differential equations into ordinary differential equations. A software, MATLAB function bvp4c is implemented to visualize the model. Sketches portraying impacts on velocities and temperature versus arising parameters are drawn and deliberated well. One of the notable findings includes that temperature of fluid is reduced by enhancing thermal stratification parameter. Moreover, drag force coefficient is evaluated for upper and lower plate in tabular form. The results demonstrate that drag force coefficient is increasing at upper plate while for lower plate it is decreasing when nanoparticles volume fraction, suction and injection values are enhanced.

TABLE OF CONTENTS

LIST OF TABLES

LIST OF FIGURES

i

NOMENCLATURE

Acronyms

Cu	Copper
CuO	Copper Oxide
Nu	Nusselt number
CC	Cattaneo-Christov
EG	Ethylene glycol

Symbols

a	constant
U_w	Stretching velocity towards wall
p^*	Modified pressure
$u, v, w,$	Velocity components
μ_{nf}	Dynamic viscosity of nanofluid
μ_{hnf}	Dynamic viscosity of hybrid nanofluid
α_{nf}	Thermal diffusivity of nanofluid
α_{hnf}	Thermal diffusivity of hybrid nanofluid
η	Similarity Variable
v_0	Uniform velocity
$\left(c_p\right)_{nf}$	Heat capacitance of nanofluid
$\left(c_p\right)_{hnf}$	Heat capacitance of hybrid nanofluid

ρ_{nf}	Density of nanofluid
ρ_{hnf}	Density of hybrid nanofluid
ρ_{s1}	Density of nanoparticle (Cu)
ρ_{s2}	Density of nanoparticle (CuO)
p	Pressure
τ	Cauchy stress tensor
$\mathbf{q}$	Heat flux density
$\mathbf{q}_t$	Steady heat flux
∇T	Temperature gradient
∇V	Velocity gradient
k_{nf}	Thermal conductivity of fluid
k_{hnf}	Thermal conductivity of hybrid fluid
k_{CNT}	Thermal conductivity of carbon nanotubes
k_{s1}	Thermal conductivity of carbon nanotubes
k_{s2}	Thermal conductivity of carbon nanotubes
k_{bf}	Thermal conductivity of carbon nanotubes
T	Temperature
T_0	Temperature at upper surface
T_h	Temperature at lower surface
b_1, b_2	Dimensional constants
ϕ	Nanoparticle volume fraction
ϕ_1	Nanoparticle volume fraction (Cu)
ϕ_2	Nanoparticle volume fraction (CuO)

β_2	Thermal relaxation time
$f'(\eta), g(\eta)$	Dimensional velocities
$\theta(\eta)$	Dimensionless temperature
Re	Reynolds number
A_2 μ_f	Rotation parameter
S	Suction/injection
S_1	Thermal stratification parameter
τ_w	Cauchy stress towards wall
C_f	Skin friction coefficient
Pr	Prandtl number
Re_x	Local Reynold number
ε_1	Ratio of heat capacitance and dynamic viscosity
ε_2	Ratio of density and dynamic viscosity
ε_3	Ratio of thermal conductivity
μ_f	Dynamic viscosity of fluid

Subscripts

f	Fluid
w	wall
nf	nanofluid
hnf	hybrid nanofluid
h	Plate difference

Chapter 1

Introduction and literature review

1.1 Introduction

Nanofluid is a collection of tiny solid particles ranging in size from 1-100nm and are suspended in base liquid such as water.These solid particles are called nanoparticles. The size of nanoparticles having diameter ranging from 100×10^{-9}. The ideal size of nanoparticles less than 20×10^{-9}. It is a fact that low thermal conductivity of basefluids do not meet the criteria of heating and cooling rates. By adding nanoparticles in basefluid heat transfer rate is triggered. Stability of nanofluids is required to enhance thermal conductivity. Most common nanomaterials are metals, carbides and oxides while base fluids are water, kerosene and ethylene glycol etc. The practical applications of nanofluids is mainly used in nuclear reactor, fuel cells and chemical industry. Due to enhancement in thermal conductivity, nanofluids plays a vital role in modern industries. The exceptional features of nanofluid include; enhancement of heat transfer and thermal conductivity with low viscosity. The structure of additives in nanofluid has a significant effect on nanofluid properties. There are two methods for the preparation of nanofluid *i.e.,* single phase (solid phase) and two phase (liquid phase). In single phase method, condensation physical vapour method is used to minimise assembling of nanoparticles to prepare Cu-ethylene glycol. This method involves dispersing of nanoparticles in a fluid. As one

step method trying to create and distributing particles in fluid at same time. Since drying, storing, transporting and dispersion of nanoparticles are neglected to minimise the agglomeration of nanoparticles and enhance stability of nanoparticles. In two phase method, chemical or physical methods are used to form fine powders of nanoparticle, nanofibers or nano materials. In the next process, nano-sized powder is dispersed into fluid with the help of high shear mixing, ball milling etc [1]. It is more economical process to make nanofluids on large scale.

Hybrid-nano particles are prepared by adding two or more nanoparticles into a base fluid. Turcu [2], a researcher who introduced concept of hybrid nanoparticles. Major step in introducing hybrid-nanofluid by Esfe et al. [3-5]. They focused on new area by balancing viscosity in hybrid- nanofluid. The aim of hybrid-nanofluids is to use physical and chemical features of two or more different kind of nano particles. Studies show the emerging characteristics of thermophysical and rheological properties. Factors affecting heat transfer strengthening of hybrid-nanofluid including selection of base fluid and size of nano particles; balancing viscosity; temperature of fluid and stability; miscibility and purification of nanoparticles. Some nano-particles possess a strong thermal behavior while other possess good rheological characteristics. They do not own all desirable features for engineering and industrial fields. For example, a nano material metallic oxide, such as Al_2O_3 is chemically stable but low thermal properties while non-metallic nano-additives *i.e.*, copper, aluminium and silver have excellent thermal conductivity however they are chemically unstable. By combining metallic nanoparticles with metallic oxides, it generate chemically stable along with thermal efficient nano-composite. Hybrid-nanofluid dynamics is progressively dominant as a result of these benefits. Its composition can be obtained by dispersing or scattering nano particles in a carrier fluid. Vehicle's radiator and generators, engine cooling mechanism and thermal storage devices etc. are of great importance of hybrid nanofluid. The unique properties of hybrid nanofluids have drawn interest of huge percentage of global research community.

In heat flow transfer analysis, stratification plays an important role. Sometimes the

mechanism of deformable density happened in the shallow fluid medium owing to change in the state of concentration, pressure, temperature and dissolved substances termed as stratification. It is witnessed that in case of stratification, density is the function of space variable as well as time. Because of which layer formation occurs. It is due to imbalance of temperature and density in fluid medium that causes thermal stratification. Common example is thermal energy from heated bodies *e.g.*, sun. Moreover temperature differences, concentration differences or by the presence of various fluids along density variations causes fluid stratification. The use of thermal stratification not only limited to natural process but also occurs in agriculture, fisheries, oceanography, chemical and geophysical flows. In thermally stratified medium, an incompressible and viscous mixed convective boundary layer flows is analyzed towards a stretching cylinder [6]. It is found from analysis that heat transfer rate at the surface of flow in thermally stratified medium is reduced as compare to unstratified medium. The nanofluid may be able to change its viscosity according to strength of magnetic field applied to it, depending on shape and size of nano materials in the presence of thermal stratification. On convective flows, it has greater impact on heat and mass transfer analysis. A significant problem on mixed convection in a double stratification is observed on boundary layer flow and transfer of heat over a vertical plate for nanofluids [7]. Such flows involves in rivers, lakes, oceans and energy storage system.

In the past, heat transfer was often discussed using Fourier's [8] law of heat conduction. The energy equation is parabolic according to Fourier's law. It demonstrates that the initial disruption has an immediate impact on the entire system. The foundation of thermal conductivity is thus provided by Fourier's law and combined with law of energy conservation it forms basis for analysis of conduction problems. From Fourier's law of heat conduction equation, it is observed that absolute temperature is important in both thermostatics and heat conduction moreover temperature gradient is merely a major factor for heat flux in linear theory. He pioneered many innovations by formulating heat conduction in terms of partial differential equation by develop methods for solving equa-

tions and envisioned problems into three steps: heat transport in space, heat storage inside element of solid and boundary conditions [9]. Besides their uses, Fourier's law has many limitations: there is no internal heat generation as conduction of heat take place under steady state and thermal conductivity does not change with time.

The anomalous behavior in Fourier law termed as "Paradox in heat conduction" which was solved by Cattaneo. Cattaneo [10] amends this law by the insertion of thermal relaxation time in Fourier's law that has been used to regulate this problem. It seems that such assumptions lead in a hyperbolic energy equation for the temperature field, which permits for the transmission by thermal waves with finite speed. The hyperbolic heat equation for temperature field is developed as a result of this modification. Furthermore, heat transmission is allowed to flow thermal waves at a finite speed. Heat transmission of this type has a wide range of practical applications ranging from nanofluid flows to skin burn injury modelling. Christov [11] amends Cattaneo by adding thermal relaxation time in order of Oldroyd's upper convected derivatives for formulation of material invariant. This model is characterized as the Cattaneo-Christov heat flux model in the literature. Various endeavors were performed after the development of Cattaneo-Christov model to validate fluid flow according to this law. The heat transfer in viscoelastic flow caused by an exponentially stretched sheet is described by this model [12]. A mathematical model is proposed to study Cattaneo-Christov heat flux for Maxwell fluid boundary layer over stretching sheet with velocity slip [13]. In an initial and boundary value problem, the uniqueness and structure stability of solutions for temperature governing Cattaneo Christov heat flow model is demonstrated by Tibullo and Zimpoli [14].

1.2 Literature Review

Nanofluids are useful in a variety of applications due to their unique features. It is mostly used in nano technologies, micro-electronics and heat transfer analysis. Choi and Eastman [15] in 1995, made a pioneering effort in nanofluids. In single phase heat transfer

liquids, nanofluids have tremendous ability for improving heat transfer properties. Based on studies and applications, Shi et al. [16] has given a brief overview on nano fluids. Nanofluids between parallel plates is common and well known problem with applications in accelerators, MHD power generator, pumps and crude oil etc. Using lattice Boltzman method Shekholeslami et al. [17] obtained a numerical solution of nanofluid in presence of magnetic field. Ramzan et al. [18] used heat and mass convective boundary conditions for Jeffery nanofluid flow over a linear stretched surface. Another factor that effects the efficiency of nanofluids is the material chosen for obtaining nano-meter sized particles. Murshad et al. [19] demonstrate that choosing right material for nanoparticles can significantly improve thermal properties of nanofluids. They used carbon nanotubes in their analysis and discover that thermal properties of nanofluids are enhanced up to six times more than standard nano-materials at room temperature. With the ever increasing demand for high performance devices, a consistent effort is expected in terms of manufacturing and development. By using multi-composites nanomaterial is most recent development in thermal enhancement. A hybrid-nanofluid is a nanofluid that contains many different forms of nanoparticles. Hybrid-nanofluid formation can obtained by dispersion of two or more nano-additives in a fluid. As a result, a resulting mixture produces a hybrid-nanofluid which can possess all chemical and physical features of nano-additives [20]. Hayat and Nadeem [21] analysed the thermal enhancement obtained by using water based (Ag-CuO) hybrid nanofluid flow past a stretching sheet. Tiwari and Das [22] discussed the enhanced thermo-physical properties using a single phase model. Devi and Devi [23] investigated for energy equation and boundary layer of hybrid-nanofluid (Cu-Al_2O_3/H_2O) over a stretching medium with different arising parameters with various assumptions for mono-nanofluid and hybrid-nanofluid. Khashi et al. [24] studied the flow and heat transfer of hybrid nanofluid past a porous shrinking cylindrical surface. A single phase nanofluid along with enhanced model of thermophysical properties are used.

The mechanism of heat transfer is necessary for temperature change between boundaries. Heat propogating mechanism has a wide range applications in industrial and

engineering purposes *i.e.,* food process, nuclear reactor, thermal transmission etc. Many scientific investigations have focused on heat transfer via convection. It plays an important role in a variety of energy related applications such as automotive radiator, lubricants and coolants in mechanical process. Malvandi et al. [25] explained asymptotic solution to stagnation phase of nanofluid flow over permeable dilating surface by using Homotopy analysis. Tsai et al. [26] studied the effects of flow and heat transfer past a time independent stretching medium with non-uniform source of heat. Hayat et al. [27] predicted a uniform density of third grade liquid with variable conductivity under the influence of C-C heat fluidity on Dracy Frochheimer flow. They noticed that with increase in Forchheimer parameter, velocity of fluid decreases. The unsteady squeezing CNTs based nanofluid flow under the influence of C-C heat flux along with homogeneous and heterogeneous reactions amidst two parallel disc is reported by Lu et al. [28]. In the second grade fluid flow past a stretching cylinder, Alamri et al. [29] focused on significance of C-C heat flux. It was reported that for large values of relaxation parameter, fluid temperature increases. The effect of adding time relaxation under C-C heat flux model to achieve equilibrium state in Tangent hyperbolic fluid flow along second order slip in heat transfer is examined by Ramzan et al. [30]. They also observed rise in fluid's velocity under the effect of Weissenberg number. Ali et al. [31] numerically reported the MHD Carreau nanofluid flow under the imapct of C-C heat flux along with a stagnation point chemical. They came up with the conclusion that velocity of fluid is decreases when a strong magnetic field source is applied. Nanofluid flow containing carbon nanotubes with Darcy Forchheimer effect related to C-C heat flux is analyzed by Ramzan and Shaheen [32].

Nanofluid flow between parallel plates has a numerous applications in engineering, industry and technology. It has a wide range applications in accelerators, automobile engines etc. The pioneering work was done by Goodman [33] who studied viscous fluid among parallel plates. Sheikoleslami et al. [34] studied three dimension viscous nanofluid flow amidst parallel plates with rotating framework along magnetohydrodynamics MHD.

Ahmed et al. [35] studied numerically the flow heat transfer mechanism of nanofluid containing carbon nanotubes in an asymmetric framework with deformable walls. Furthermore, several researchers have investigated various phenomena including different geometries *i.e.*, dilating and squeezing in nanofluids. A rotation is present in nature of fluid flow at some level. Vajravelua and Kumar et al. [36] reported MHD viscous fluid flow amidst two horizontal parallel plates, where one plate is stretched while other one is porous. They found a numerical solution and examined the impact of physical parameters. Hayat et al. [37] used various models to investigate non-Newtonian fluid flow with rotation and used extended work using two or three dimensions. Mehmood and Ali [38] used an analytical approach to viscous three dimensional fluid flow over rectangular medium with the help of Homotopy Analysis approach between parallel plates where lower wall is stretched bi-directional and upper wall is permeable. Mehmood et al. [39] extended their previous research work by considering suction and injection effects for both walls and transport of mass phenomena. They also observed the effects of viscous drag force and thermal transfer process. Hussain and Ali [40] reported three dimensional viscous fluid flows of second grade in a rotating frame. They examined the behaviour of certain parameters on velocity distribution. Lu et al. [41] discussed hybrid-nanofluid flow under the effect of non-linear thermal radiation, heat generation entropy minimization. They also examined the effect of mass and thermal transport. The observation of hybrid nanofluid flow behavior by using (Cu-CuO/water) under the effect thermal radiation and Hall current is observed in a rotating frame work is examined by [42]. This proposed model is enhanced under the impact of MHD effect. Sheikoleslami et al. [43] investigated viscous nanofluid flow in three dimensional amidst parallel plates along rotating framework under the effect of magneto-hydro dynamics (MHD). In the presence of radiation effect, Eldabe et al. [44] identified the MHD visco-elastic fluid flow past a horizontal stretching sheet in a permeable medium. Hayat et al. [45] studied the water based (Ag-CuO) hybrid nanofluid past a stretching medium and identify the thermal benefits by using hybrid- nanofluid flow.

Based on above discussion, it is observed that flow of hybrid-nanofluid consisting of Cu and CuO with ethylene glycol as base fluid under the effect of Cattaneo-Christov heat diffusion amidst two parallel plates are not discussed in literature yet. The aim of this study is to fill this gap and resolve the problem of C-C heat diffusion with thermal stratification in rotating framework where upper plate is porous and lower plate is stretching with variable velocity. Impacts of prominent parameters for drag force coefficient are portrayed in tabular form. Numerical solutions of present work is obtained by adopting bvp4c built in function of MATLAB scheme.

Chapter 2

Preliminaries

This chapter is consists of certain perceptions, definitions and fundamental laws.

2.1 Fluid

A fluid is a material that deforms continuously when a shear stress or external force is applied. Liquid, gases and plasmas are examples of fluids.

2.2 Nanofluid

A fluid that comprises of nanometer-sized particles is called nanofluid. Metals, oxides and carbides are widely used as nanofluid. Enhancement of heat transfer and electrical conductivity is main application of nanofluid.

2.3 Hybrid-Nanofluid

Hybrid nanoparticles are defined as nanoparticles composed by two or more distinct materials of nanoscale size. The fluids created with hybrid nanoparticles are known as hybrid nanofluids.

2.4 Fluid mechanics

It is a branch of physics that describes behavior of fluid *i.e.*, in motion or at rest. It is divided into two classes:

2.4.1 Fluid statics

It is a branch of fluid mechanics that deals with behavior of fluid's particles at rest.

2.4.2 Fluid dynamics

It is a branch of fluid mechanics that deals with behavior of fluid's particles in motion.

2.5 Flow

A flow is a material that deforms under the impact of different forces. It is categorised into two classes:

2.5.1 Laminar flow

It is a type of flow in which velocity remains constant and behavior of fluid flow is uniform at each step.

2.5.2 Turbulent flow

It is a type of flow in which velocity varies at each step and behavior of fluid flow changes spontaneously.

2.6 Viscosity

It is a basic property of fluid that defines resistance of fluid flow when several forces acting on it. It is divided into two classes:

2.6.1 Dynamic viscosity

A resistance to movement of one layer of fluid to another is known as dynamic viscosity. Mathematically, it is defined as:

$$\mu = \frac{\tau}{du/dy}. \tag{2.1}$$

A unit of μ is $(kg/m.s)$, in S.I units having dimension $[M\ /LT]$.

2.6.2 Kinematic viscosity

It is defined as ratio of dynamic viscosity μ to density ρ. Mathematically , it is defined as:

$$\nu = \frac{\mu}{\rho}. \tag{2.2}$$

It's unit is m^2/s having dimension$[L^2/T]$.

2.7 Rotating frame

A rotating frame of reference is a type of non-inertial reference frame that revolves around an inertial reference frame. A surface of earth is the typical example of rotating frame.

2.8 Shear stress

It is defined as force that tends to distort a material by causing it to slip across a plane or a plane parallel to applied stress.

2.9 Newton's law of viscosity

It is defined as shear stress in a flowing fluid is directly proportional to the rate of velocity gradient. Newton's law of viscosity is mathematically written as:

$$\tau \propto (du/dy)\,, \tag{2.3}$$

or

$$\tau = k(du/dy). \tag{2.4}$$

in which τ denotes shear stress applied on fluid's element and μ is proportionality constant.

2.10 Newtonian fluids

A fluid that follows Newton's law of viscosity is known as Newtonian fluid. There is a linear relation among viscosity μ and shear stress τ. Water, oil and glycerin etc. are common examples of Newtonian fluids.

2.11 Non-Newtonian fluids

A fluid that does not follows Newton's law of viscosity is known as non-Newtonian fluids. When a shear stress is applied to them, viscosity of fluid varies. Mathematically, it is written as:

$$\tau \propto (du/dy)^N, \quad N \neq 1. \tag{2.5}$$

$$\tau = K(du/dy)^N. \tag{2.6}$$

Equation(2.6) is changes to Newton's law of viscosity when $K = \eta$, and $N = 1$

$$\tau = \eta(du/dy), \qquad \eta = K(du/dy)^{N-1}. \tag{2.7}$$

where η is apparent viscosity, N the flow behavior index, and K is consistency index. Fluids like toothpaste, honey, ketchup etc are examples of non-Newtonian fluids.

2.12 Density

A substance density is defined as ratio of mass per unit volume. Mathematically, it is stated as:

$$\rho = \frac{m}{V}. \tag{2.8}$$

Its unit is kg/m^3 with dimensions $[M/L^3]$.

2.13 Pressure

It is a ratio of applied force F to surface area A. Mathematically,

$$P = \frac{F}{A}. \tag{2.9}$$

Its unit is N/m.

2.14 Porous surface

A surface with holes that allows outside material pass through it. Some common examples of porous surface include, sponge fabric and cardboard.

2.15 Permeability

An intensity of spongy material that allows fluid to pass through it. Surfaces having large holes are highly permeable.

2.16 Stratification

The phenomenon of particles deposition into layers under the effect of temperature change and mixture of various fluids having different densities, is termed as startification. The importance of stratification in convection transportmechanism reasoned to its extensive applications in industrial, natural and engineering fluids.

2.17 Thermal Stratification

Thermal stratification arises due to variation in temperature which enhanced density variation in the fluid medium. The fluid expands and contracts during heating and cooling which causes variation in density. The fluid stratification due to variation in the temperature caused by radiating heated sheet e.g, vertical plate, and curved sheet etc.

2.18 Heat flux

A flow of energy per unit area and time is known as heat flux or thermal flux. Mathematically,

$$q = -k\left(\nabla T\right). \tag{2.10}$$

where k is thermal conductivity, ∇T is temperature gradient . As above equation called Fourier's Law. Its unit in S.I is $W/sq.m^2$.

2.19 Fourier Law

A law of heat conduction is known as Fourier's law which states that a rate of heat transfer through a substance is proportional to negative gradient in temperature and region at normal to that gradient through which heat flows.

$$q = -k\left(\nabla T\right). \tag{2.11}$$

where q is local heat flux density, k =material's conductivity, ∇T =Temperature's gradient. The above expression is Fourier's law in one dimension.

2.20 Cattaneo-Christov heat flux

It is adaptation of Fourier's law by two mathematicians Cattaneo [10] and Christov [11] Mathematicaly, it is stated as:

$$\mathbf{q} + \boldsymbol{\lambda}_2\left(\mathbf{q}_t + \mathbf{V}.\boldsymbol{\nabla}\mathbf{q} - \mathbf{q}.\boldsymbol{\nabla}\mathbf{V} + \left(\boldsymbol{\nabla}.\mathbf{V}\right)\mathbf{q}\right) = -\mathbf{k}\boldsymbol{\nabla}\mathbf{T}. \tag{2.12}$$

where λ_2 is thermal relaxation time, $\mathbf{q}$ is heat flux, k is thermal conductivity and ∇T is temperature gradient.

2.21 Heat transfer Mechanism

A mechanism that transport energy and entropy from one position to another. It include thermal radiation convection and conduction.

2.21.1 Conduction

In the mechanism of heat transfer, heat flows from hot to cold region due to collision of molecules in solids and liquids. In mathematical form,

$$Q = -kA\nabla T = -kA\left[\frac{dt}{dx}\right], \tag{2.13}$$

where negative sign indicates that heat is conducted from higher to lower temperature. Q represents heat flow, A is surface area, k is thermal conductivity $\frac{dt}{dx}$ denotes temperature gradient where negative sign indicates that heat is conducted form high to lower temperature.

2.21.2 Convection

In the mechanism of heat transfer, heat flows from hot to cold region due to collision of moecules in gases and liquids. In mathematical form

$$Q = -hA\nabla T. \tag{2.14}$$

where h is convective heat transfer coefficient, A surface area and ∇T is temperature gradient.

2.21.3 Radiation

The absorption or transmission of energy in the form of waves or particles across space or material medium is known as radiation.

$$Q = E\sigma^* A(\triangle T^4), \tag{2.15}$$

or

$$Q = E\sigma^* A(T_1^4 - T_2^4), \tag{2.16}$$

or

$$Q = E\sigma^* A(T_2^4 - T_1^4), \tag{2.17}$$

or

$$q = \frac{Q}{A} = -E\sigma^*(T_2^4 - T_1^4). \tag{2.18}$$

where q denotes heat transfer, E is emissivity of the system, σ for constant Stephan Boltzman A for area, where $(\triangle T^4)$ is temperature difference of fourth power.

2.22 Coriolis force

The coriolis force is a hypothetical inertial force that acts on moving objects in a frame of reference that rotates with repect to inertial frame reference.

$$F_c = 2m(\Omega \times V). \tag{2.19}$$

where m is mass, Ω is angular velocity and V is velocity.

2.23 Centripetal force

A force that acts on a body moving in a circular direction and directed towards body's centre of rotation.

$$F_c = \frac{mv^2}{r}. \tag{2.20}$$

where F_c Centriperal force, m is mass, v is velocity and r is radius.

2.24 Centrifugal force

A force that arising from the body's inertia, which appears to act on a body moving in a circular path and is directed away from the centre around which the body is moving.

$$F = m\omega^2 r$$

where, m is mass, ω is angular velocity and r is radius.

2.25 Conservation laws

A conservation law states that a particular measurable attributes remains uniform when a physical structure alter over time. The law that deals with conserved quantity is called conservation laws. Some fundamentals laws are given below:

2.25.1 Mass conservation law

This law states that in any closed system, whole mass is conserved. Mathematically

$$\frac{D\rho}{Dt} + \rho(\nabla.V) = 0, \tag{2.21}$$

$$\frac{D\rho}{Dt} + (\nabla.V)\rho + \rho(\nabla.V) = 0, \tag{2.22}$$

$$\frac{\partial\rho}{\partial t} + \nabla.(\rho V) = 0, \tag{2.23}$$

which is called continuity equation. In case of steady flow, (ρ=constant) Equation (2.19) becomes

$$\nabla.(\rho V) = 0, \tag{2.24}$$

for incompressible flow

$$(\nabla.V) = 0. \tag{2.25}$$

2.25.2 Momentum conservation law

This law states that in any closed system whole momentum is conserved . Mathematically

$$\boldsymbol{\rho}\frac{DV}{Dt}=\operatorname{div}\boldsymbol{\tau}_c+\boldsymbol{\rho}\mathbf{B}_f, \tag{2.26}$$

where τ denotes cauchy stress tensor and B denotes body force.

$$\tau_c = -PI + \mu A_1. \tag{2.27}$$

2.25.3 Energy conservation law

This law states that in any closed system whole energy is conserved. Mathematically,

$$(\rho C_p)\frac{DT}{Dt}=\boldsymbol{\tau}_c\acute{\mathbf{L}}-\mathbf{divq}+\boldsymbol{\rho}\mathbf{D}_E, \tag{2.28}$$

where q and $\acute{L}$ are:

$$q = -k\nabla T, \tag{2.29}$$

$$\acute{L} = \nabla V, \tag{2.30}$$

and for this law τ_c is

$$\tau_c = -PI + \mu A_1, \tag{2.31}$$

with

$$A_1 = L + L^T. \tag{2.32}$$

.

2.26 Non-dimensional numbers

2.26.1 Skin friction coefficient (C_{f_r})

A quantity of a drag force experienced by a fluid when it pass through a surface. It occurs between liquid and dense surface, reducing fluid flow's rate. Mathematically, it is written as:

$$C_{f_r} = \frac{\tau_w}{(1/2)\rho U_w}. \tag{2.33}$$

where τ is shear stress towards wall, ρ is density and U_w is velocity.

2.26.2 Nusselt number (Nu)

A ratio of conductive to convective heat transfer at a fluid's boundary is known as Nusselt number. Mathematically

$$N_L = \frac{h^* \triangle T}{k \triangle T} = \frac{h^* l}{k}. \tag{2.34}$$

where h represent convective heat transfer l represents characteristics length and k for thermal conductivity.

2.26.3 Prandtl number (Pr)

It describes a ratio of momentum diffusivity to thermal diffusivity. Mathematically

$$Pr = \frac{\upsilon}{\alpha} = \frac{\mu C_P}{k}. \tag{2.35}$$

in which μ denotes dynamic viscosity, C_p denotes specific heat and k denotes thermal conductivity. In heat transfer, Prandtl number is used to control the thickness of momentum and thermal boundary layer.

2.26.4 Reynolds number (Re)

It is a non-dimensional number that defines as ratio of inertial to viscous forces. It is used to determine flow type *i.e.*, laminar or turbulent. At low Reynold number indicates laminar flow where viscous effects are prevalent while high Reynold number shows turbulent flow where inertials effects are prevalent. Mathematically

$$Re = \frac{Inertial force}{Viscous force} = \frac{\rho \upsilon L}{\mu}. \tag{2.36}$$

where υ is velocity of fluid, L is characteristic length and μ is dynamic viscosity.

2.27 Suction and injection

When region of sytem pressure is reduced as compare to other,the fluid in higher region exerts pressure which is known as suction. The insertion of liquid and gases under pressure into fluid is known as injection. Suction/injection is used to control flow of a fluid.

2.28 Thermal relaxation parameter

It is dimensionless widely used parameter for calcuating amount of time it takes for heat conduction.

2.29 Thermal conductivity (k)

The thermal conductivity of a substance is a measure of its ability of heat conduction. It is property of heat flows and a distance per unit area and temperature gradient. Mathematically

$$k = \frac{Qd}{A \triangle T}. \tag{2.37}$$

where Q is heat transfer rate, d is material of unit thickness, A unit cross sectional area and $\triangle T$ is temperature difference. In S.I system thermal conductivity has unit $\frac{W}{m.k}$ and dimensions is $\left(\frac{ML}{T^3\theta}\right)$.

2.30 Thermal diffusivity (α)

The thermal diffusivity is defined as a ratio of thermal conductivity per unit density and specific heat capacity. Mathematically

$$\alpha = \frac{k}{\rho C_p}. \tag{2.38}$$

where k is thermal conductivity, ρ is density and C_p is specific heat capacity.

2.31 Specific heat capacity (C_p)

The amount of heat added per mass required to increase a temperature of substance at a pressure by 1K. Mathematically, it is written as,

$$C_p = \frac{Q}{m\nabla T}. \tag{2.39}$$

where C_p is Specific heat capacity of pressure, Q is energy, m is mass and ∇T change is temperature.

Chapter 3

Onset of Cattaneo-Christov heat flux and thermal stratification in ethylene-glycol based nanofluid flow containing carbon nanotubes in a rotating frame

In this chapter, steady flow of rotating nano-fluid ethylene glycol based single-walled (SW) and multi-walled (MW) carbon nanotubes (CNTs) between two parallel plates under the influence of Cattaneo-Christov (C-C) heat flux is studied. Apart from above, impact of thermal stratification is also considered. Furthermore, effect of coriolis force and centripetal force are accompained with fluid's rotation. The required boundary layer equations are converted into non-linear ordinary differential equations with the help of suitable similarity transformations. MATLAB's function, bvp4c approach is used to address the arising problem. The result of arising parameters versus velocity and temperature profiles are drawn and analyzed.

3.1 Mathematical formulation

Let consider an incompressible flow of ethylene glycol consist of single-walled and multi-walled carbon nanotubes in a rotating frame passing amidst two parallel plates with an angular velocity $\Omega = [0, \Omega, 0]$. The upper plate is porous while lower plate is stretched with variable velocity $U_w = ax$ where$(a > 0)$. The steady state velocity is expressed as $V[u(x, y), v(x, y), w(x, y)]$ with (u, v, w) are velocity components in (x, y, z) directions. Figure 3.1 shows flow plan of envisioned model and Table 3.1 shows the thermophysical properties of SWCNTs, MWCNTs and ethylene glycol.

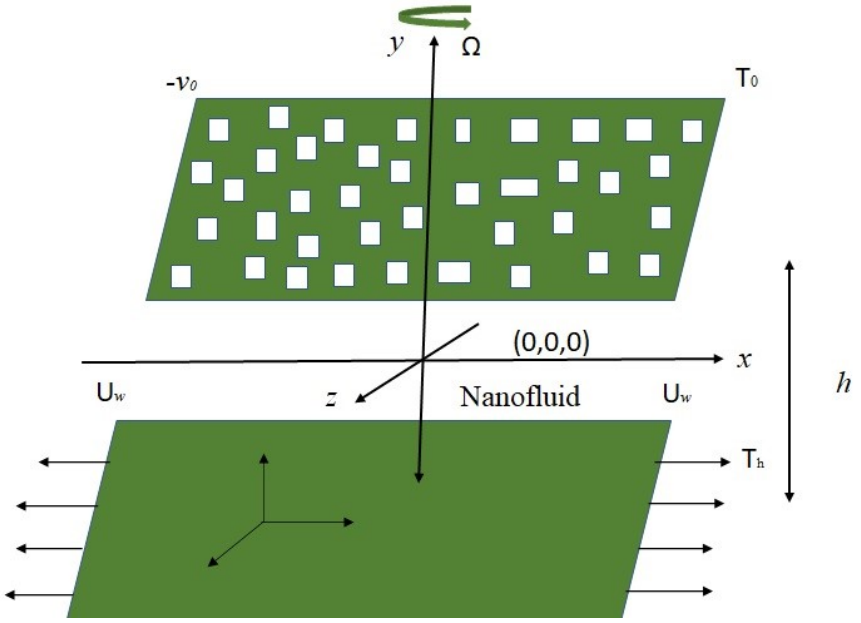

Fig. 3.1 Rotating fluid framework

The equation of momentum for rotating flow is follow [46] as :

$$\boldsymbol{\rho}_{nf}\left(\frac{dV}{dt}+\mathbf{2\Omega}\times\mathbf{V}+\mathbf{\Omega}\times(\mathbf{\Omega}\times\mathbf{r})\right)=\text{div}\,\mathbf{T}. \tag{3.1}$$

The coriolis and centrifugal forces are represented by components $(\mathbf{2\Omega}\times\mathbf{V})$ and $(\mathbf{\Omega}\times(\mathbf{\Omega}\times\mathbf{r}))$. Continuity equation is given as:

$$u_x + v_y = 0. \tag{3.2}$$

The equation of momentum written in component form is given as:

$$\rho_{nf}\left(uu_x + vu_y + 2\Omega w\right) = -\frac{\partial p^*}{\partial x} + \mu_{nf}(u_{xx} + u_{yy}), \tag{3.3}$$

$$\rho_{nf}(uv_x + vv_y) = -\frac{\partial p^*}{\partial y} + \mu_{nf}(v_{xx} + v_{yy}), \tag{3.4}$$

$$\rho_{nf}(uw_x + vw_y - 2\Omega u) = \mu_{nf}(w_{xx} + w_{yy}). \tag{3.5}$$

Here in equations (3.2)-(3.4) modified pressure is represented as:

$$p^* = p - \frac{\Omega^2 x}{2} \tag{3.6}$$

The non-presence term $\frac{\partial p*}{\partial z}$ in (3.5) depicts net flow distribution in z-direction. The notion of heat transfer equation is given below:

$$(\rho c_p)(uT_x + vT_y) = -\nabla.\mathbf{q}, \tag{3.7}$$

and heat flux equation written as:

$$\mathbf{q} + \boldsymbol{\lambda}_2(\mathbf{q}_t + \mathbf{V}.\nabla\mathbf{q} - \mathbf{q}.\nabla\mathbf{V} + (\nabla.\mathbf{V})\mathbf{q}) = -\mathbf{k}\nabla\mathbf{T}. \tag{3.8}$$

Eliminating $\mathbf{q}$ [11] from (3.6) and (3.7), we get

$$uT_x + vT_y = \frac{k_{nf}}{(\rho c)_{nf}}T_{yy} - \lambda_2 \begin{pmatrix} u^2T_{xx} + v^2T_{yy} + 2uvT_{xy} \\ +\left(uu_x + vu_y\right)T_x + \left(uv_x + vv_y\right)T_y \end{pmatrix} \tag{3.9}$$

The boundary conditions for above problem are as follows:

$$
\begin{aligned}
u &= U_w = ax, \quad v = 0, \quad w = 0, \quad T = T_h = T_0 + b_1 x \quad at \quad y = 0, \\
u &= 0, \quad v = -v_0, \quad w = 0, \quad T = T_0 = T_0 + b_2 x \quad at \quad y = h.
\end{aligned} \tag{3.10}
$$

Where, $v_0 > 0$ is suction and $v_0 < 0$ is injection.

The thermophysical characteristics for carbon nanotubes and nanofluid are given below where density and heat capacitance model is presented by Pak and Co-workers [47].

$$\rho_{nf} = (1-\phi)\rho_f + \phi\rho_{CNT}, \tag{3.11}$$

$$(\rho c)_{nf} = (1-\phi)(\rho c)_f + \phi(\rho c)_{CNT}, \tag{3.12}$$

The density model for nanofluid is proposed by Brinkman [48] and Xue [49] proposed a model of thermal conductivity given as:

$$\mu_{nf} = \frac{\mu_f}{(1-\phi)^{2.5}}, \qquad \alpha_{nf} = \frac{k_{nf}}{(\rho c)_{nf}}, \tag{3.13}$$

$$k_{nf} = k_f \left(\frac{1 - \phi + 2\phi \left(\frac{K_{CNT}}{K_{CNT} - K_f} \right) \ln \left(\frac{K_{CNT} + K_f}{2k_f} \right)}{1 - \phi + \phi \left(\frac{K_{CNT}}{K_{CNT} - K_f} \right) \ln \left(\frac{K_{CNT} + K_f}{2k_f} \right)} \right). \tag{3.14}$$

Table 3.1 shows the thermophysical properties ρ (density), C_p (specific heat), k (thermal conductivity) of ethylene glycol (base fluid) and carbon nanotubes [51].

Physical Properties	Ethylene glycol	SWCNT	MWCNT
$\rho\left(\frac{kg}{m^3}\right)$	1115	2600	1600
$C_p\left(\frac{J}{kg.K}\right)$	2430	425	796
$\mathrm{K}\left(\frac{W}{m.K}\right)$	0.253	6600	3000

3.1.1 Similarity tansformations

Non-dimensional similarity tansformation are given as:

$$u = axf'(\eta), \quad v = -ahf(\eta), \quad w = axg(\eta), \qquad \theta(\eta) = \frac{T - T_0}{T_h - T_0}, \qquad \eta = \frac{y}{h}. \tag{3.15}$$

following ordinary differential equations are as follows

$$f^{iv} + \mathrm{Re}\,\varepsilon_2(f'f'' - ff''') - 2A_2\varepsilon_2 g' = 0, \tag{3.16}$$

$$g'' - \mathrm{Re}\,\varepsilon_2(gf' - fg') + 2A_2\varepsilon_2 f' = 0, \tag{3.17}$$

$$\theta''\left(\frac{\varepsilon_3}{\varepsilon_1 \,\mathrm{Pr}\,\mathrm{Re}} - \beta_2 f^2\right) + 2\beta_2 ff'\theta' - \beta_2 f'^2\theta$$
$$-\beta_2 S_1 f^2 + \beta_2 ff''\theta + \beta_2 S_1 ff'' + f\theta' - f'\theta - f'S_1 = 0 \tag{3.18}$$

and the boundary conditions are as follows:

$$\begin{aligned} f(0) &= 0, \qquad g(0) = 0, \qquad \theta(0) = 1 - S_1, \qquad f'(0) = 1, \\ f(1) &= S, \qquad g(1) = 0, \qquad \theta(1) = 0, \qquad f'(1) = 0 \end{aligned} \tag{3.19}$$

Numerical Strategem:

From equations (14) to (16) with aforementioned boundary condictions (17), are converted into ordinary differential equations by employing MATLAB built in function bvp4c in order to originate numerical code. Initial estimation with tolerance of 10^{-6} is used for subjeted numerical scheme. Without interupting the solution approach, initial approximations must satisfy booundary conditions.

$$
\begin{aligned}
f &= y_1, \quad f' = y_2, \quad f'' = y_3, \quad f''' = y_4, \quad f^{iv} = yy_1, \\
yy_1 &= 2A_2\varepsilon_2 y_6 - \mathrm{Re}\,\varepsilon_2\left(y_2^2 - y_1 y_3\right), \\
g &= y_5, \qquad g' = y_6, \qquad g'' = yy_2, \\
yy_2 &= \mathrm{Re}\,\varepsilon_2\left(y_5 y_2 - y_1 y_6\right) - 2A_2\varepsilon_2 y_2, \\
\theta &= y_7, \; \theta' = y_8, \quad \theta'' = yy_3, \\
yy_3 &= -\left(\frac{1}{\frac{\varepsilon_3}{\varepsilon_1 \mathrm{Pr}\,\mathrm{Re}} - \beta_2 y_1^2}\right)\left(\begin{array}{c} 2\beta_2 y_1 y_2 y_8 - \beta_2 y_2^2 y_7 - \beta_2 S_1 y_2^2 + \beta_2 y_1 y_3 y_7 \\ +\beta_2 S_1 y_1 y_3 + y_1 y_8 - y_2 y_7 - y_2 S_1 \end{array}\right)
\end{aligned} \tag{3.20}
$$

Dimensionless Parameters:

$$\varepsilon_3 = k_f\left(\frac{1-\phi+2\phi\left(\frac{K_{CNT}}{K_{CNT}-K_f}\right)\ln\left(\frac{K_{CNT}+K_f}{2k_f}\right)}{1-\phi+\phi\left(\frac{K_{CNT}}{K_{CNT}-K_f}\right)\ln\left(\frac{K_{CNT}+K_f}{2k_f}\right)}\right),$$

$$\alpha_{nf} = \frac{k_{nf}}{(\rho c)_{nf}},$$

$$\varepsilon_2 = \frac{\rho_{nf}}{\mu_{nf}},$$

$$\varepsilon_1 = \left[(1-\phi) + \phi\frac{(\rho c_p)_{CNT}}{(\rho c_p)_f}\right](1-\phi)^{2.5},$$

$$S = \frac{v_0}{ah}, \qquad \mathrm{Re} = \frac{ah^2}{v_f}, \qquad A_2 = \frac{\Omega h^2}{v_f}, \qquad S_1 = \frac{b_2}{b_1}, \quad \beta_2 = a\lambda_2 \tag{3.21}$$

Where as Re is Reynolds number, A_2 is rotation parameter, S is suction/injection, S_1 is thermal stratification parameter, ε_3 is ratio of thermal conductivity, ε_2 is ratio of density and dynamic viscosity. ε_1 is ratio of heat capacitance and dynamic viscosity where β_2 is thermal relaxation parameter. The surface drag force in dimensional form are:

$$
\begin{aligned}
C_f &= \frac{\tau_w}{(1/2)\rho_{nf}U_w^2}, \qquad where \quad \tau_w = \mu_{nf}\left(\frac{\partial u}{\partial y}\right)|_{y=0} \quad and \\
\tau_w &= \mu_{nf}\left(\frac{\partial u}{\partial y}\right)|_{y=1}
\end{aligned} \tag{3.22}
$$

The heat transfer rate in dimensional form are:

$$
\begin{aligned}
Nu &= \frac{hq_w}{k_f\left(T_h - T_0\right)}, \qquad where \qquad q_w = -k_{CNT}\left(\frac{\partial T}{\partial y}\right)|_{y=0,} \qquad and \\
q_w &= -k_{CNT}\left(\frac{\partial T}{\partial y}\right)|_{y=1,}
\end{aligned} \tag{3.23}
$$

Non-dimensional components of drag force and heat transfer rate at lower plate are given below:

$$
(1/2)C_f\sqrt{\mathrm{Re}_x} = \frac{f\,''(\eta)}{\left((1-\phi)+\phi\frac{\rho_{CNT}}{\rho_f}\right)(1-\phi)^{2.5}}|_{\eta=0,} \tag{3.24}
$$

$$
Nu = -\frac{k_{CNT}}{k_f}\theta(\eta)\,|_{\eta=0}, \tag{3.25}
$$

Non-dimensional components of drag force and heat transfer rate at upper plate are given below:

$$
(1/2)C_f\sqrt{\mathrm{Re}_x} = \frac{f\,''(\eta)}{\left((1-\phi)+\phi\frac{\rho_{CNT}}{\rho_f}\right)(1-\phi)^{2.5}}|_{\eta=1,} \tag{3.26}
$$

$$
Nu = -\frac{k_{CNT}}{k_f}\theta(\eta)\,|_{\eta=1} \tag{3.27}
$$

where local Reynold number is,

$$
\mathrm{Re}_x = \frac{hU_w}{v_f}.
$$

3.2 Results and discussions

Results are exemplify for velocities $f'(\eta), g(\eta)$ and temperature $\theta(\eta)$ against arising parameters such as thermal stratification (S_1), suction/injection (S), Reynolds number (Re), Rotation parameter (A_2). Using bvp4c software, issues are numerically analysed.Results are considered for single-walled and multi-walled carbon nanotubes. Fig. 3.2 and fig. 3.3 are drawn to see the relation between both velocities and nanoparticle volume fraction ϕ. Opposite trend of velocities against nanoparticle volume fraction is observed and noticed that nanoparticle volume fraction ϕ aginst two velocities are increased for both carbon nanotubes. Moreover, it alter more quickly in Single-walled as compared to multi-walled. In case of suction($-v_0 > 0$) and injection ($-v_0 < 0$), fig. 3.4 and fig.3.5 shows that velocities are increased for S . It is observed that influence of velocity is increase in middle as compare to upper and lower plates. For$S > 0$, highest velocity is slightly moved towards lower plate and it alters for $S < 0$. Fig. 3.6 and fig. 3.7 illustrates the trend of Re against velocity profiles. From fig. 3.6, it depicts that velocity is moving from increasing to decreasing at mean position due to stretching of lower plate. Fig. 3.7 shows a significant reduction in velocity versus a higher estimate value of Re. This is due to the fact that velocity will constant at center of plate while lower plate is in static condition but with rising value of Re, velocity will be shifted at bottom plate. Fig. 3.8 and fig. 3.9 shows behavior A_2 against both velocities. In fig. 3.8, velocity change is double folded in a limited domain. With domain $0 \leq \eta \leq 0.5$, velocity is decrease while velocity is increases with domain $0.5 \leq \eta \leq 1.0$. It is therefore, noted that velocity is more prevalent in upper half of domain than lower half. Figure 3.10 depicts the effect of thermal stratification parameter S_1 on temperature profile. It is clear from graph that fluid temperature is reduced by increasing value of S_1. Large value of S_1 causes reduction in temperature difference between upper and lower plate. Table 3.2 and Table 3.3 reveals the behavior of skin friction coefficient and heat transfer rate for various value of suction / injection S and nanoparticle volume fraction ϕ in single-walled and multi-walled by fixing Reynolds number Re and rotation parameter A_2 for $\eta = 0$ and $\eta = 1$. It is observed that trend

for SWCNTs similar to MWCNTs for S and A_2. For large values of nanoparticle ϕ and from $S = 0 \leq 1$, drag force coefficient is increased near upper plate and decrease near lower plate.

Table 3.2 Numerical values of drag force $(1/2)\mathrm{C}_f.\,\mathrm{Re}_x^{1/2}$versus different values of parameter for SWCNT

$S\downarrow$	$\phi\downarrow$	$(1/2)\mathrm{C}_f\,\mathrm{Re}_x^{1/2}$ at $\eta = 0$			
		$A_2 = 0$		$A_2 = 1$	
		$\mathrm{Re} = 0.5$	$\mathrm{Re} = 1$	$\mathrm{Re} = 0.5$	$\mathrm{Re} = 1$
-0.5	0.0	-6.94643	-6.8922	-6.9805	-6.9292
-0.5	0.1	-7.9851	-7.9311	-8.0146	-7.9627
-0.5	0.2	-9.6027	-9.5488	-9.6270	-9.5744
-1	0.0	-9.7349	-9.4681	-9.7970	-9.5416
-1	0.1	-11.2190	-10.9525	-11.2720	-9.6472
-1	0.2	-13.5299	-13.2638	-13.5730	-13.3123
0	0.0	-4.0428	-4.0856	-4.0532	-4.0959
0	0.1	-4.6364	-4.6792	-4.6454	-4.6882
0	0.2	-5.5607	-5.6035	-5.5682	-5.6110

$S\downarrow$	$\phi\downarrow$	$(1/2)\mathrm{C}_f\,\mathrm{Re}_x^{1/2}$ at $\eta=1$			
		$A_2=0$		$A_2=1$	
		$\mathrm{Re}=0.5$	$\mathrm{Re}=1$	$\mathrm{Re}=0.5$	$\mathrm{Re}=1$
-0.5	0.0	5.1070	5.2184	5.1286	5.2412
-0.5	0.1	5.8487	5.9592	5.8674	5.9788
-0.5	0.2	7.0037	7.1133	7.0192	7.1294
-1	0.0	8.3863	8.8089	8.4315	8.8575
-1	0.1	9.5712	9.9866	9.6102	10.0281
-1	0.2	11.4173	11.8246	11.4494	11.8584
0	0.0	1.9764	1.9532	1.9759	1.9529
0	0.1	2.2732	2.2499	2.2727	2.2496
0	0.2	2.7353	2.7119	2.7349	2.7116

Table 3.3 Numerical value of drag force $(1/2)\mathrm{C}_f\,\mathrm{Re}_x^{1/2}$ versus different values of parameters for MWCNT.

S	ϕ	$(1/2)\mathrm{C}_f\,\mathrm{Re}_x^{1/2}$ at $\eta = 0$			
		$A_2 = 0$		$A_2 = 1$	
		$A_1 = 0.5$	$A_1 = 1$	$A_1 = 0.5$	$A_1 = 1$
-0.5	0.0	-6.9463	-6.8922	-6.9805	-6.9292
-0.5	0.1	-8.6760	-8.6221	-8.7030	-8.6508
-0.5	0.2	-11.1962	-11.1423	-11.2168	-11.1640
-1	0.0	-9.7349	-9.4681	-9.7970	-9.5416
-1	0.1	-12.2061	-11.9398	-12.2544	-11.9949
-1	0.2	-15.8064	-15.5405	-15.8428	-15.5808
0	0.0	-4.0428	-4.0856	-4.0532	-4.0959
0	0.1	-5.0312	-5.0740	-5.0395	-5.0823
0	0.2	-6.4713	-6.5141	-6.4777	-6.5205

S	ϕ	$(1/2)\mathrm{C}_f\,\mathrm{Re}_x^{1/2}$ at $\eta = 1$			
		$A_2 = 0$		$A_2 = 1$	
		$\mathrm{Re} = 0.5$	$\mathrm{Re} = 1$	$\mathrm{Re} = 0.5$	$\mathrm{Re} = 1$
-0.5	0.0	5.1070	5.2184	5.1286	5.2412
-0.5	0.1	6.3420	6.4521	6.3592	6.4700
-0.5	0.2	8.1417	-8.2506	8.1549	8.2642
-1	0.0	8.3863	-8.8089	8.4315	8.8575
-1	0.1	10.3596	10.7712	10.3954	10.8090
-1	0.2	13.2366	13.6383	13.2640	13.6669
0	0.0	1.9764	1.9532	1.9759	1.9529
0	0.1	2.4706	2.4472	2.4701	2.4469
0	0.2	3.1905	3.1671	3.1902	3.1668

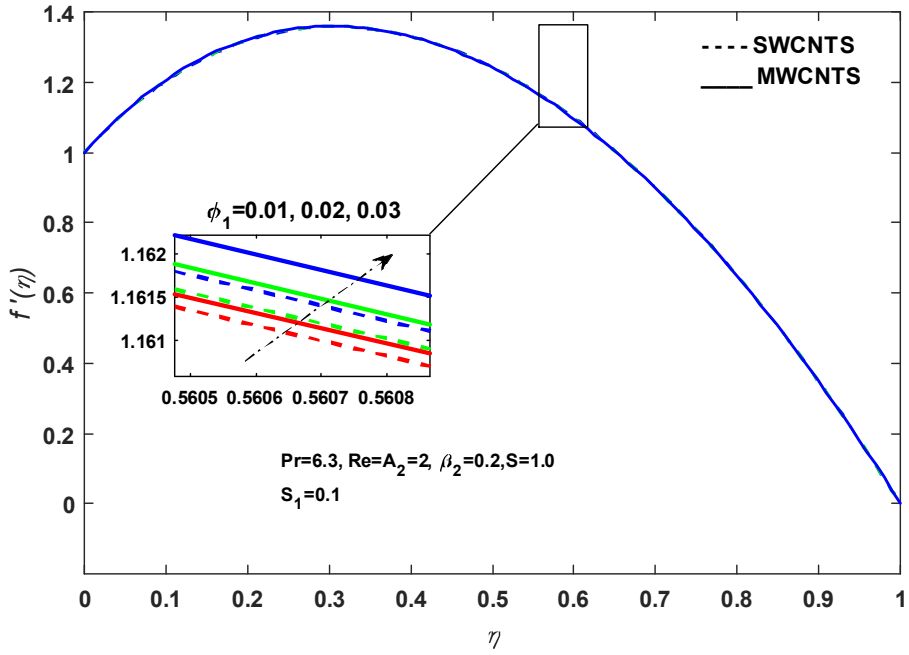

Fig. 3.2 Change in f′ (η) $vs.\phi$

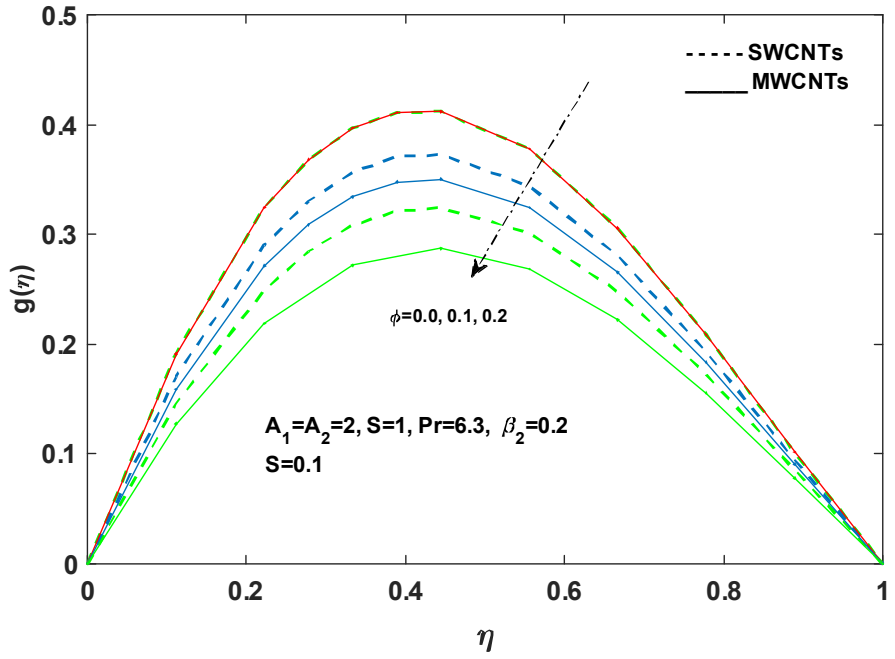

Fig. 3.3 Change in g(η) vs. ϕ

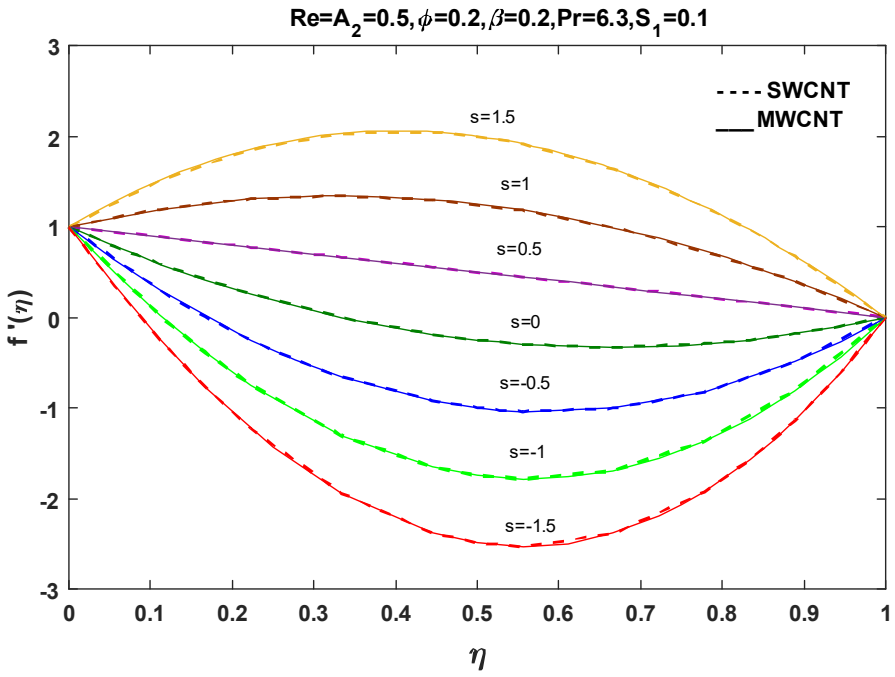

Fig. 3.4 Change in f′ (η) vs. S

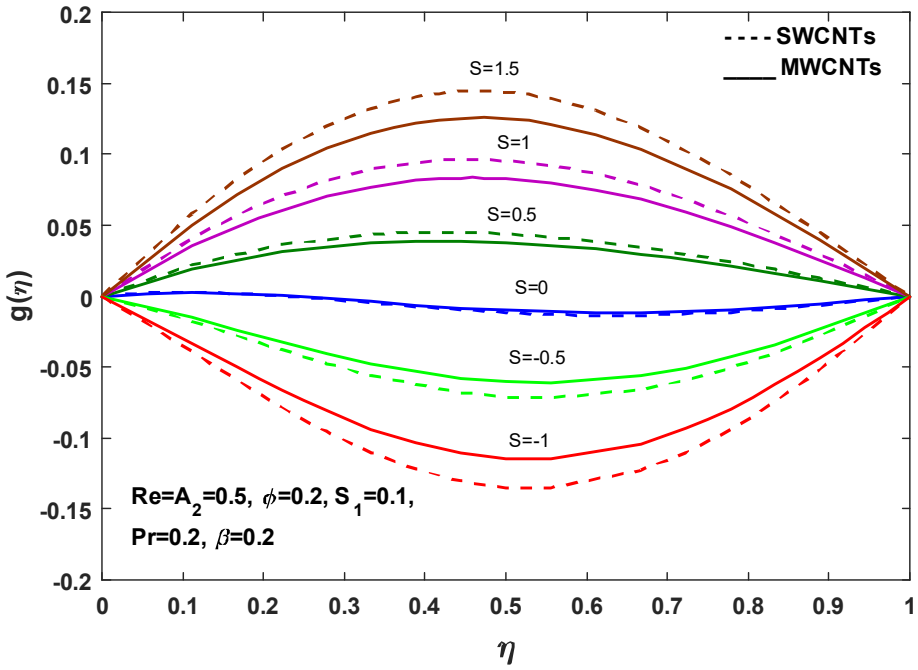

Fig. 3.5 Change in g(η) vs. S

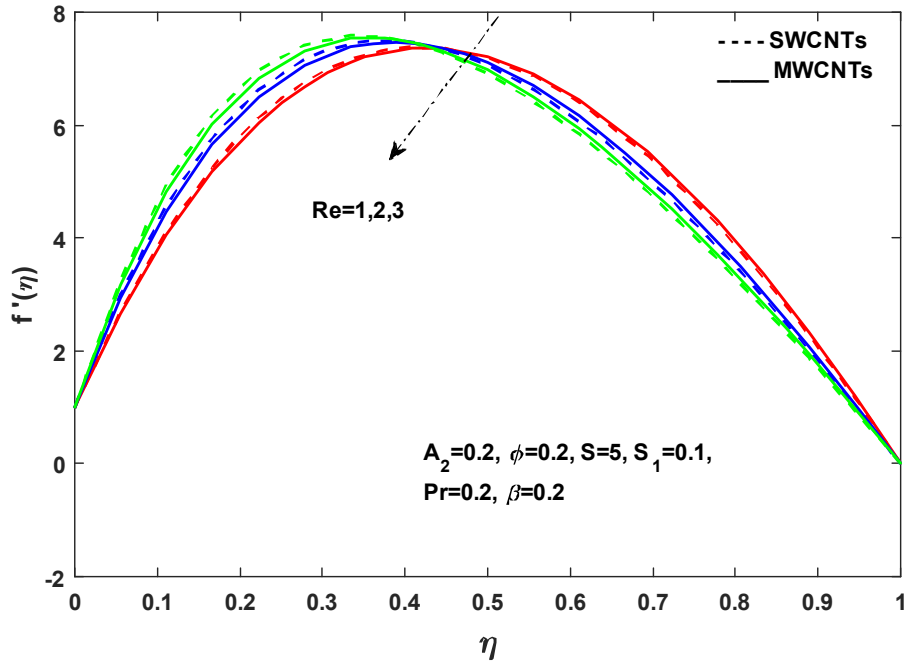

Fig. 3.6. Change in f′ (η) vs. Re

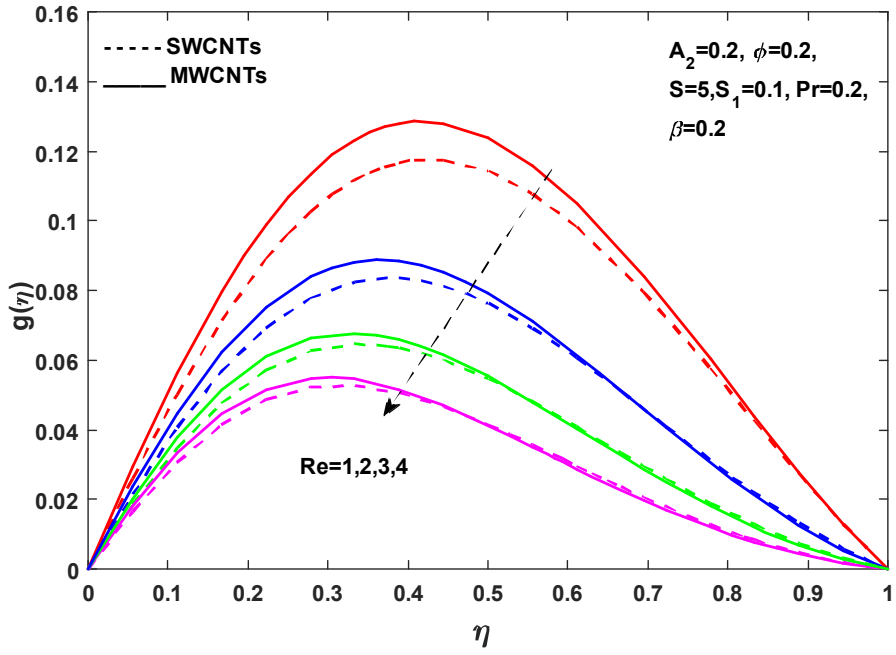

Fig. 3.7 Change in g(η) vs. Re

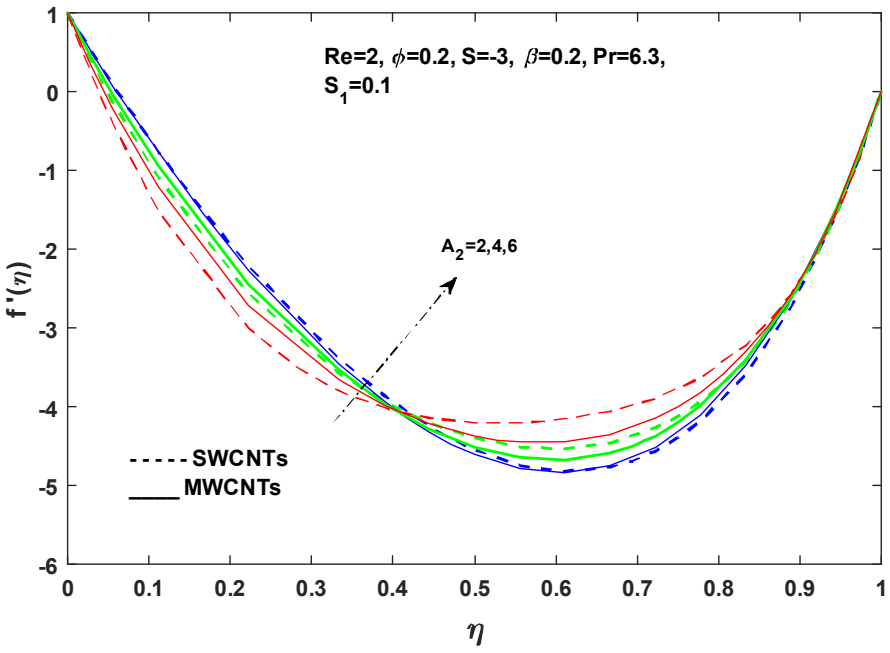

Fig. 3.8 Change in f′ (η) vs. A_2

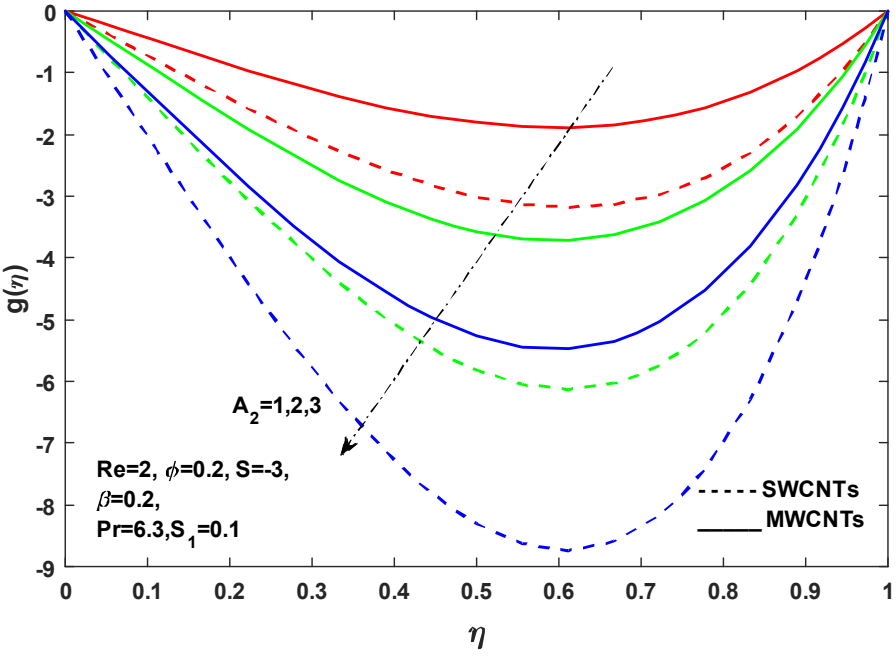

Fig. 3.9 Change in g(η) vs. A_2

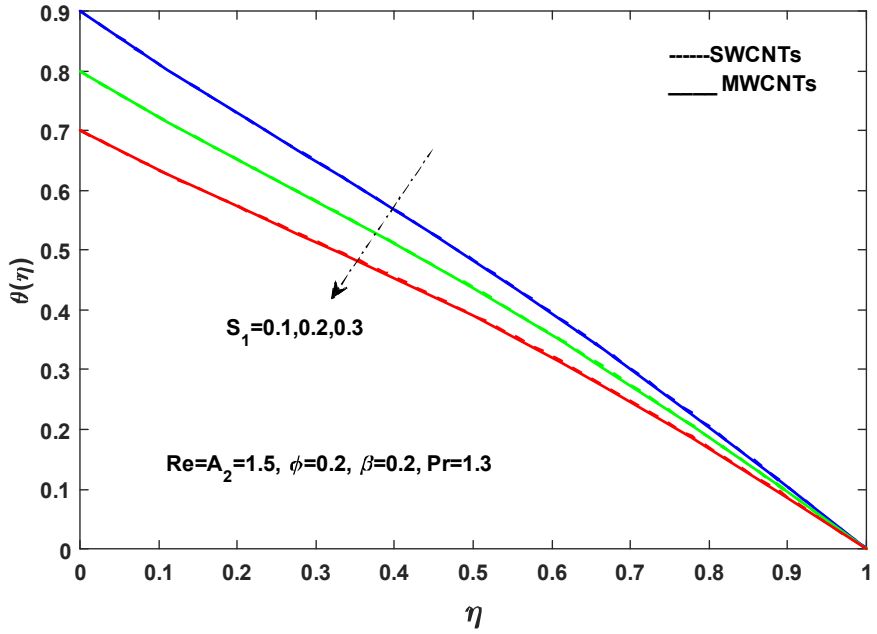

Fig. 3.10 Change in $\theta(\eta)$ vs. S_1

Chapter 4

Hybrid nanofluid flow with modified Fouriers law in a rotating frame

In this chapter we intend to examine the behavior of ethylene glycol based hybrid nanofluid flow containing copper (Cu) and copper oxide (CuO) between two parallel plates in a rotating frame whose upper plate is permeable while lower one is stretched along x-axis under the effect of Cattaneo-Christov heat flux. The influence of thermal stratification is also analyzed. Moreover, the effects of coriolis force along with centripetal force is analyzed with fluid's rotation. By applying similarity transformations, non-dimensional ordinary differential equations are derived. MATLAB's built in function bvp4c is used for set of ordinary differential equations. The impacts of the arising parameters against velocity and temperature profiles are drawn and analyzed. It is discerned that temperature is declined for rising values of thermal stratification parameter while for Reynold number it shows increasing behavior.

4.1 Mathematical modelling

Consider a viscid steady flow of ethylene glycol based hybrid nanofluid containing Copper(Cu) and Copper Oxide (CuO) nanoparticles between parallel plates with constant angular velocity Ω along y-direction in a frame. The distance between parallel plates is represented by h. The upper wall is permeable while lower wall is stretched with a variable velocity $U_w = ax$. The steady velocity is denoted by $V = [u(x, y), v(x, y), w(x, y)]$ along (x, y, z) directions. Fig4.1 depicts the flow pattern of the subject fluid flow and Table 4.1 shows the thermophysical properties of nanoparticles (Cu and CuO) and base fluid (Ethylene glycol).

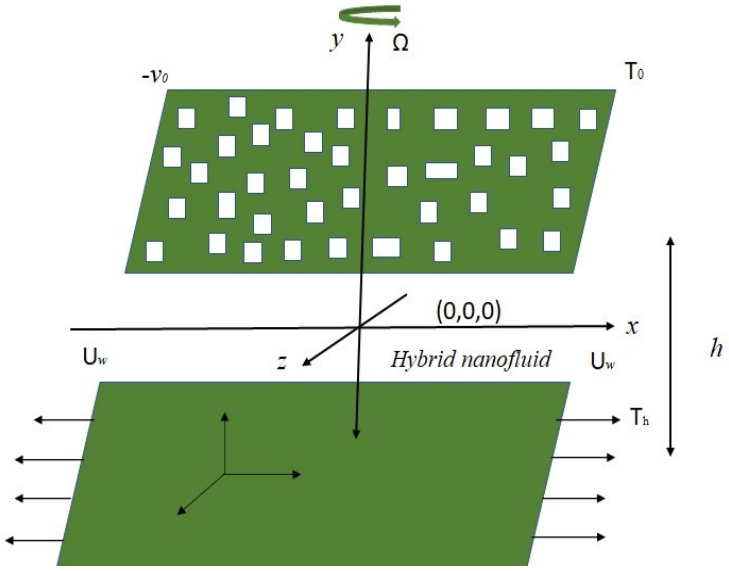

Fig. 4.1 Rotating fow framework

The equation of momentum for rotating flow is follow as [46]

$$\rho_{hnf}\left(\frac{dV}{dt} + (\mathbf{2\Omega} \times \mathbf{V}) + (\mathbf{\Omega} \times (\mathbf{\Omega} \times \mathbf{r}))\right) = \text{div}\,\mathbf{T}. \tag{4.1}$$

The coriolis and centrifugal forces are represented by components$(\mathbf{2\Omega} \times \mathbf{V})$ and $\mathbf{\Omega} \times (\mathbf{\Omega} \times \mathbf{r})$.

Continuity equation is given as:

$$u_x + v_y = 0 \tag{4.2}$$

The equation of momentum written in component form is given as:

$$\rho_{hnf}\left(uu_x + vu_y + 2\Omega w\right) = -\frac{\partial p^*}{\partial x} + \mu_{hnf}(u_{xx} + u_{yy}), \tag{4.3}$$

$$\rho_{hnf}\left(uu_x + vu_y\right) = -\frac{\partial p^*}{\partial y} + \mu_{hnf}(v_{xx} + v_{yy}), \tag{4.4}$$

$$\rho_{hnf}\left(uu_x + vu_y + 2\Omega w\right) = \mu_{hnf}(w_{xx} + w_{yy}). \tag{4.5}$$

Here in equations (4.2)-(4.4) modified pressure is represented as:

$$p^* = p - \frac{\Omega^2 x}{2}, \tag{4.6}$$

The nonpresence term $\frac{\partial p*}{\partial z}$ in (4.5) depicts net flow distribution in z-direction. The notion of heat transfer equation is given below:

$$\left(\rho c_p\right)\left(uT_x + vT_y\right) = -\nabla.\mathbf{q}, \tag{4.7}$$

where T is local fluid temperature which satisfies the following heat flux equation [45]:

$$\mathbf{q} + \boldsymbol{\lambda}_2(\mathbf{q}_t + \mathbf{V}.\nabla\mathbf{q} - \mathbf{q}.\nabla\mathbf{V} + (\nabla.\mathbf{V})\mathbf{q}) = -\mathbf{k}\nabla\mathbf{T}, \tag{4.8}$$

Eliminate $\mathbf{q}$ from (4.6) and (4.7), following [11]

$$uT_x + vT_y = \frac{k_{hnf}}{(\rho c_p)_{hnf}} T_{yy} - \lambda_2 \begin{pmatrix} u^2T_{xx} + u^2T_{yy} + 2uvT_{xy} \\ + \left(uu_x + vu_y\right)T_x + \left(uv_x + vv_y\right)T_y \end{pmatrix} \tag{4.9}$$

.

The boundary conditions for above problem are given as follow:

$$\begin{aligned} u &= U_w = ax, \quad v = 0, \quad w = 0, \quad T = T_h = T_0 + b_1 x \quad at \quad y = 0. \\ u &= 0, \quad v = -v_0, \quad w = 0, \; T = T_0 = T_0 + b_2 x \quad at \quad y = h. \end{aligned} \tag{4.10}$$

Where, $v_0 > 0$ is suction and $v_0 < 0$ is injection.

The thermophysical characteristics for hybrid -nanofluid are given below where density and heat capacitance model for hybrid nanofluid is presented by Pak and Co-workers [47].

$$\rho_{hnf} = (1 - \phi_2) \left[(1 - \phi_2)\rho_f + \phi_1 \rho_{s1} \right] + \phi_2 \rho_{s2}, \tag{4.11}$$

$$(\rho c_p)_{hnf} = (1 - \phi_2) \left[(1 - \phi_2)\rho_f + \phi_1 (\rho c_p)_{s1} \right] + \phi_2 (\rho c_p)_{s2},$$

The density model for nanofluid is proposed by Brinkman [48] and Maxwell [50] proposed a model of thermal conductivity given as:

$$\mu_{hnf} = \frac{\mu_f}{(1 - \phi_1)^{2.5}(1 - \phi_2)^{2.5}}, \qquad \alpha_{hnf} = \frac{k_{hnf}}{(\rho c)_{hnf}}, \tag{4.12}$$

$$\begin{aligned} k_{hnf} &= k_{bf} \left(\frac{k_{s2} + 2k_{bf} - 2\phi_2 (k_{bf} - k_{s2})}{k_{s2} + 2k_{bf} + \phi_2 (k_{bf} - k_{s2})} \right), \\ k_{bf} &= k_f \left(\frac{k_{s1} + 2k_{bf} - 2\phi_1 (k_{bf} - k_{s1})}{k_{s1} + 2k_{bf} + \phi_2 (k_{bf} - k_{s1})} \right) \end{aligned} \tag{4.13}$$

Table 4.1 shows the thermophysical properties ρ (density), C_p (specific heat), k (thermal conductivity) of ethylene glycol (base fluid), Cu and CuO (Nano particles) [52].

Physical Properties	Ethylene glycol	Cu	CuO
$\rho\left(\frac{kg}{m^3}\right)$	1115	8933	6500
$C_p\left(\frac{J}{kg.K}\right)$	2430	385	540
$\mathrm{K}\left(\frac{W}{m.K}\right)$	0.253	401	18

4.1.1 Similarity tansformations

Non dimensional similarity transformation are given as

$$u = axf'(\eta), \quad v = -ahf(\eta), \qquad w = axg(\eta), \quad \theta(\eta) = \frac{T - T_0}{T_h - T_0}, \qquad \eta = \frac{y}{h}. \tag{4.14}$$

obtaining governing equations are:

$$f^{iv} + \mathrm{Re}\,\varepsilon_2^*(f'f'' - ff''') - 2A_2\varepsilon_2^* g' = 0, \tag{4.15}$$

$$g'' - \mathrm{Re}\,\varepsilon_2^*(gf' - fg') + 2A_2\varepsilon_2^* f' = 0, \tag{4.16}$$

$$\theta''\left(\frac{\varepsilon_3^*}{\varepsilon_1^*\,\mathrm{Pr}\,\mathrm{Re}} - \beta_2 f^2\right) + 2\beta_2 ff'\theta' - \beta_2 f'^2\theta$$
$$-\beta_2 S_1 f^2 + \beta_2 ff''\theta + \beta_2 S_1 ff'' + f\theta' - f'\theta - f'S_1 = 0, \tag{4.17}$$

following boundary conditions are as follows:

$$\begin{aligned} f(0) &= 0, \qquad g(0) = 0, \qquad \theta(0) = 1 - S_1, \qquad f'(0) = 1, \\ f(1) &= S, \qquad g(1) = 0, \qquad \theta(1) = 0, \qquad f'(1) = 0\ . \end{aligned} \tag{4.18}$$

Dimensionless parameters are mentioned below:

$$
\begin{aligned}
\varepsilon_3^* &= k_f \left(\frac{k_{s2} + 2k_{bf} - 2\phi_2(k_{bf} - k_{s2})}{k_{s2} + 2k_{bf} + \phi_2(k_{bf} - k_{s2})} \right) \left(\frac{k_{s1} + 2k_{bf} - 2\phi_1(k_{bf} - k_{s1})}{k_{s1} + 2k_{bf} + \phi_2(k_{bf} - k_{s1})} \right). \\
\varepsilon_2^* &= (1 - \phi_2) \left[\left((1 - \phi_1) \rho_f + \phi_1 \rho_{s1} \right) + \phi_2 \rho_{s2} \right] (1 - \phi_1)^{2.5} (1 - \phi_2)^{2.5}, \qquad (4.19) \\
\varepsilon_1^* &= (1 - \phi_2) \left[\left((1 - \phi_2) \rho_f + \phi_1 (\rho c_p)_{s1} \right) + \phi_2 (\rho c_p)_{s2} \right], \\
S &= \frac{v_0}{ah}, \qquad \mathrm{Re} = \frac{ah^2}{v_f}, \qquad A_2 = \frac{\Omega h^2}{v_f}, \qquad S_1 = \frac{b_2}{b_1}, \qquad \beta_2 = a\lambda_2
\end{aligned}
$$

Where as Re is Reynold numbers, A_2 is rotation parameter, S is suction/injection, S_1 is thermal stratification parameter, ε_3^* is ratio of thermal conductivity, ε_2^* is ratio of density and dynamic viscosity. ε_1^* is ratio of heat capacitance and dynamic viscosity where β_2 is thermal relaxation parameter. Drag force and heat transfer rate in dimensional form are:

$$
\begin{aligned}
C_f &= \frac{\tau_w}{(1/2)\rho_{hnf}.U_w^2}, \qquad where \qquad \tau_w = \mu_{hnf} \left(\frac{\partial u}{\partial y} \right) |_{y=0}, \ and \\
\tau_w &= \mu_{hnf} \left(\frac{\partial u}{\partial y} \right) |_{y=0} \qquad (4.20)
\end{aligned}
$$

Heat transfer in dimensional form is follow as:

$$
\begin{aligned}
Nu_x &= \frac{hq_w}{k_f (T_h - T_0)}, \quad where \qquad q_w = -k_{hnf} \left(\frac{\partial T}{\partial y} \right) |_{y=0,} \qquad and \\
q_w &= -k_{hnf} \left(\frac{\partial T}{\partial y} \right) |_{y=1,} \qquad (4.21)
\end{aligned}
$$

Non dimensional components of surface drag force and heat transfer rate at lower plate is given as:

$$
\begin{aligned}
(1/2)C_f\sqrt{\mathrm{Re}_x} &= \frac{f\,''(\eta)}{(1-\phi_2)\left[\left((1-\phi_1)\,\rho_f+\phi_1\rho_{s1}\right)+\phi_2\rho_{s2}\right](1-\phi_1)^{2.5}(1-\phi_2)^{2.5}}|_{\eta=0}.\\
Nu &= -\frac{k_{hnf}}{k_f}\theta'(\eta)\ \ |_{\eta=0} \qquad (4.22)
\end{aligned}
$$

Non dimensional components of surface drag force and heat transfer rate at upper plate is given as:

$$
\begin{aligned}
(1/2)C_f\sqrt{\mathrm{Re}_x} &= \frac{f\,''(\eta)}{(1-\phi_2)\left[\left((1-\phi_1)\,\rho_f+\phi_1\rho_{s1}\right)+\phi_2\rho_{s2}\right](1-\phi_1)^{2.5}(1-\phi_2)^{2.5}}|_{\eta=1}.\\
Nu_x &= -\frac{k_{hnf}}{k_f}\theta'(\eta)\ |_{\eta=1} \qquad (4.23)
\end{aligned}
$$

where local Reynolds number is

$$\mathrm{Re}_x = \frac{hU_w}{\upsilon_f}.$$

4.2 Results and discussions

In this section, the outcomes are portrayed against velocity profiles $f\,'(\eta)$, $g(\eta)$ and temperature profile $\theta(\eta)$ to discuss heat transport and trend of fluid flow parameters at different values. Impact of different arising parameters such as Reynold number Re, Rotation parameter A_2, suction / injection parameter S, thermal stratification parameter S are analyzed graphically. Nanofluid (Cu/EG) and hybrid nanofluid (Cu-CuO/EG), consequences are drawn. In fig.4.2 (a and b) shows the trend of velocity $f\,'(\eta)$ versus nanoparticle volume fraction ϕ_1. It shows a opposite trend of ϕ_1 against velocity for nanofluid and hybrid nanofluid. It decreases for nanofluid and increases for hybrid nanofluid due to variation in concentration of nano-composition (Cu-CuO/EG). In fig.

4.3 shows the trend of velocity $g(\eta)$ against nanoparticle volume fraction ϕ for both mono and hybrid nanofluid. It shows increasing trend in both nanofluid and hybrid nanofluid. It is noted that velocity is enhanced for $g(\eta)$ in both nanofluid and hybrid nanofluid. Although, it changes more instantly in case of nanofluid than hybrid nanofluid. Fig. 4.4 and figure 4.5, shows the trend of both velocities ($f'(\eta)$ and $g(\eta)$) against suction ($-v_0 > 0$) and injection ($-v_0 < 0$). It is observed for increasing velocity for different values of S. It is comprehended that velocity is increasing for higher value of S and velocity is decreasing for low values of S. As compared to nearby upper and lower plates, it is more prominent in centre. Fig. 4.6 and fig. 4.7, shows the trend of both velocities against Reynold number Re in both mono and hybrid nanofluid. In fig. 4.6 it is interpreted that behavior of velocity from rising to falling at mean position of a plate due to stretching of bottom plate. In fig. 4.7, shows the continuous decrease in veocity is depicted against high estimated values of Reynold number. It is due to consistent velocity at mean position of plates because bottom plate is in stagnant position. When values of Re rises, direction of velocity is shifted towards lower plate. Fig.4.8 and fig. 4.9 shows the trend of rotation parameter A_2 against both velocities in mono and hybrid nanofluid. From fig. 4.8, it is depicted that velocity shifts are two-folded in form with minimal domain.With $0 \leq \eta \leq 0.5$ domain velocity tends to decrease while it shows opposite behavior with domain $0.5 \leq \eta \leq 1.0$. Fig. 4.9, shows that velocity in upper half is more prominent as compared to lower half for both mono and hybrid nanofluid. A decreasing trend is seen for thermal stratification parameter S_1 versus temperature profile $\theta(\eta)$ in fig. 4.10 for mono and hybrid nanofluid. It is noted that, for increasing value of $(S_1 = 0.1, 0.2, 0.3)$ temperature is decreases. Large values of S_1shows the difference between parallel plates causes temperature to decline. Hence temperature of fluid is observed due to increasing value of S_1. Moreover for mono nanofluid, temperature shows lesser than hybrid nanofluid due to injection at upper wall. Fig. 4.11(a and b), shows the behavior of Reynolds number Re versus temperature profile $\theta(\eta)$ for mono and hybrid nanofluid. For$(Cu - EG)$ temperature is decreases for escalating values of Reynolds

number Re. This is due to reason that for large Re it enhances rotation profiles between parallel plates. As augmentation in Re, causes inertial forces to reduce temperature. For hybrid nanofluid, an increasing values of Re causes decrease in temperature as viscous effects become prominent which minimizes the friction effect between plates and fluid and as a result temperature decreases. Fig. 4.12(a and b) shows the opposite trend of suction/injection S in mono and hybrid nanofluid versus temperature profile $\theta(\eta)$. It shows a decreasing behavior of temperature for rising values of S and increases for decreasing value of S in mono nanofluid. As suction draws the fluid near the surface, reducing the thickness of the thermal boundary layer, whereas injection has the contrary impact. For hybrid nanofluid, temperature is increases for $S > 0$, and temperature is decreases for $S < 0$ as high velocity is shifted towards bottom plate but trend is reverse for upper plate. Moreover, increment in S shows thickness in thermal boundary layer increases as a result thermal transfer's rate also rises which causes temperature to increase. In fig. 4.13(a and b), depicts the nature of Prandtl number Pr versus temperature profile $\theta(\eta)$ in mono nanofluid and hybrid nanofluid. For mono naofluid it is decreases due to reduction in thermal boundary layer. For hybrid nanofluid it also shows decreasing behavior against temperature profile $\theta\,(\eta)$ because thermal boundary layer thickness decreaseses by increasing Pr and as a result reduces heat transfer rate so temperature decreases. Here, temperature is decreases for increasing value of Pr. In fig. 4.14 (a and b) shows trend of rotation parameter A_2 versus temperature profile $\theta(\eta)$ in mono and hybrid nanofluid. It depicts decrease in temperature for mono nanofluid and increases for hybrid nanofluid for rising values of rotation parameter. Fig. 4.15 (a and b) depicts the behavior of temperature $\theta(\eta)$ against thermal relaxation time β_2 for both (Cu-EG) and hybrid nanofluid. For (Cu-EG) and for hybrid nanofluid it is decreasing for augmented values of thermal relaxation time. Due to the large value of β_2 the behavior of nanoparticles is immensely conducting, and it consumes more time to transfer heat to neighboring particles. Fig. 4.16 (a and b) shows the trend of temperature versus nanoparticle volume fraction. For both mono and hybrid nanofluid its shows a rising behavior. As temperature profiles are

enhanced when nanoparticle volume fractions are increased. Since nanofluid's thermal conductivity rises with suspension of more nanoparticles into base fluid which in turn augments heat transfer. With the increase in heat transfer, augmentation in thickness of thermal boundary layer happens and it leads to rise in temperature Table 4.2 and 4.3, depicts the behavior of drag force coefficient by fixing values of Reynolds number Re and rotation paramter A_2 for various values of S for hybrid nanofluid. It is clear from graph, at $\eta = 0,\ S = -2, \leq 0$, drag force coefficient is increases and decreases for mounting values of ϕ_1 and fixing ϕ_2 at upper and lower plate of a wall. Similar case is observed with $\eta = 1$, at upper and lower plate drag force coefficient is rises and falling. Table 4.4 and Table 4.5shows the heat transfer rate effect for lower and upper plate on arising parameters.

Table 4.2 Numerical values of drag force $C_f \operatorname{Re}_x^{1/2}$versus different values for hybrid nanofluid by fixing ϕ_1=0.02

S	ϕ_2	$(1/2)C_f \operatorname{Re}_x^{1/2}$ at $\eta = 0$			
		A_2=0		A_2=1	
		Re =0.5	Re =1	Re =0.5	Re =1
–1	0.01	-9.0705	-8.8036	-9.1378	-8.8841
-1	0.02	-9.1915	-8.9246	-9.2578	-9.0038
-1	0.03	-9.3223	-8.9522	-9.3875	-9.1332
-0.5	0.01	-6.4813	-6.4272	-6.5181	-6.4673
-0.5	0.02	-6.5659	-6.5118	-6.6022	-6.5513
-0.5	0.03	-6.6575	-6.6034	-6.6933	-6.6423
0	0.01	-3.7771	-3.8198	-3.7882	-3.8310
0	0.02	-3.8255	-3.8682	-3.8346	-3.8792
0	0.03	-3.8778	-3.9205	-3.8886	-3.9314

S	ϕ_2	$(1/2)C_f\,\mathrm{Re}_x^{1/2}$ at $\eta = 1$			
		A_2=0		A_2=1	
		Re =0.5	Re =1	Re =0.5	Re =1
–1	0.01	7.8561	8.2828	7.9048	8.3354
-1	0.02	7.9526	8.3785	8.0006	8.4303
-1	0.03	8.0570	8.4821	8.1043	8.5331
-0.5	0.01	4.7750	4.8869	4.7983	4.9115
-0.5	0.02	4.8354	4.9472	4.8584	4.9715
-0.5	0.03	4.9008	5.0125	4.9234	5.0364
0	0.01	1.8435	1.8204	1.8430	1.8201
0	0.02	1.8677	1.8446	1.8672	1.8443
0	0.03	1.8939	1.8707	1.8933	1.8704

Table 4.3 Numerical value of drag force $C_f \operatorname{Re}_x^{1/2}$ versus different values of parameters for hybrid nanofluid by fixing $\phi_2 = 0.01$

S	ϕ_1	$C_f . \operatorname{Re}_x^{1/2}$ at $\eta = 0$			
		A_2=0		A_2=1	
		Re =0.5	Re =1	Re =0.5	Re =1
–1	0.02	-9.0705	-8.8036	-9.1378	-8.8842
-1	0.04	-8.5098	-8.2428	-8.5823	-8.3306
-1	0.06	-8.0879	-7.8207	-8.1647	-7.9149
-0.5	0.02	-6.4813	-6.4272	-6.5181	-6.4673
-0.5	0.04	-6.0888	-6.0347	-6.1282	-6.0778
-0.5	0.06	-5.7935	-5.7393	-5.8350	-5.7851
0	0.02	-3.7771	-3.8198	-3.7882	-3.8310
0	0.04	-3.5529	-3.5956	-3.5646	-3.6074
0	0.06	-3.3841	-3.4268	-3.3965	-3.4393

S	ϕ_1	$(1/2)C_f.\,\mathrm{Re}_x^{1/2}$ at $\eta = 1$			
		A_2=0		A_2=1	
		Re =0.5	Re =1	Re =0.5	Re =1
–1	0.02	7.8561	8.2828	7.9048	8.3354
-1	0.04	7.4089	7.8395	7.4609	7.8960
-1	0.06	7.0724	7.5063	7.1273	7.5662
-0.5	0.02	4.7750	4.8869	4.7983	4.9115
-0.5	0.04	4.4948	4.6072	4.5197	4.6336
-0.5	0.06	4.2840	4.3968	4.3102	4.4247
0	0.02	1.8435	1.8204	1.8430	1.8201
0	0.04	1.7314	1.7083	1.7309	1.7081
0	0.06	1.6471	1.6240	1.6465	1.6238

Table 4.4 Effect of arising parameters on Nusselt number at lower plate

Re	A_2	β_2	S_1	ϕ_2	S	Nu_x at $\eta = 0$
0.5	2.0	0.2	1.0	0.02	0	2.3695
0.5	2.0	0.2	1.0	0.04	0	1.0750
0.5	2.0	0.2	1.0	0.06	0	0.6373
1.0	2.0	0.2	1.0	0.02	0.5	4.1887
1.0	2.0	0.2	1.0	0.04	0.5	1.9035
1.5	2.0	0.2	1.0	0.06	0.5	2.7364
2.5	2.0	0.2	1.5	0.02	-1	1.0733
2.5	2.0	0.2	1.5	0.04	-1	2.1272
2.5	2.0	0.2	1.5	0.06	-1	1.7971

Table 4.5 Effect of arising parameters on Nusselt number at upper plate

Re	A_2	β_2	S_1	ϕ_2	S	Nu_x at $\eta = 1$
1.5	2.0	1.0	1.0	0.02	0	1.4159
1.5	2.0	1.0	1.0	0.04	0	0.3459
1.5	2.0	1.0	1.0	0.06	0	0.1614
1.5	2.0	1.5	2.0	0.02	0.5	1.9597
1.5	2.0	1.5	2.0	0.04	0.5	3.0450
1.5	2.0	1.5	2.0	0.06	0.5	2.9731
2.0	2.0	1.5	2.0	0.02	-0.5	2.6428
2.0	2.0	1.5	2.0	0.04	-0.5	3.4611
2.0	2.0	1.5	2.0	0.06	-0.5	2.8133

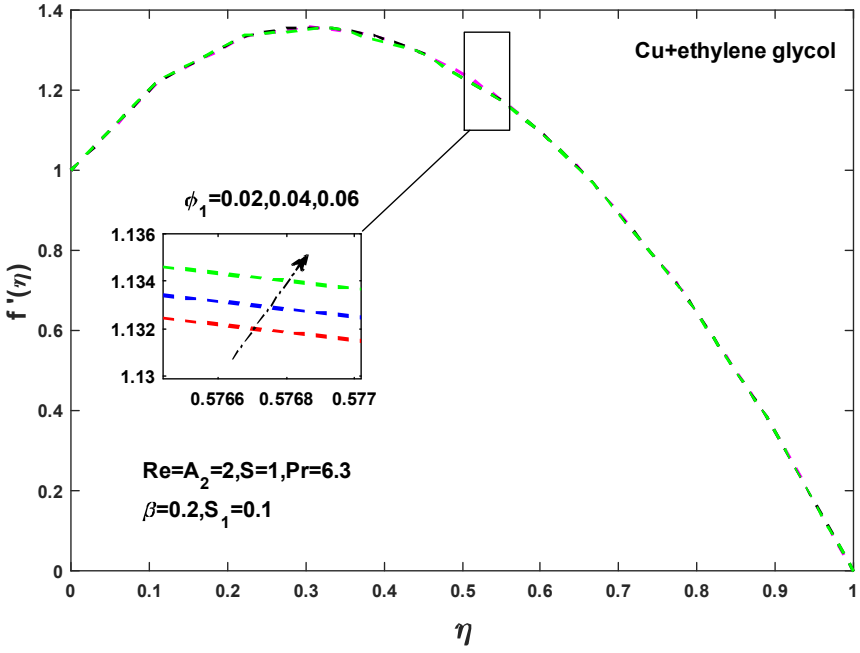

Fig. 4.2(a) Change in f′ (η) vs. ϕ

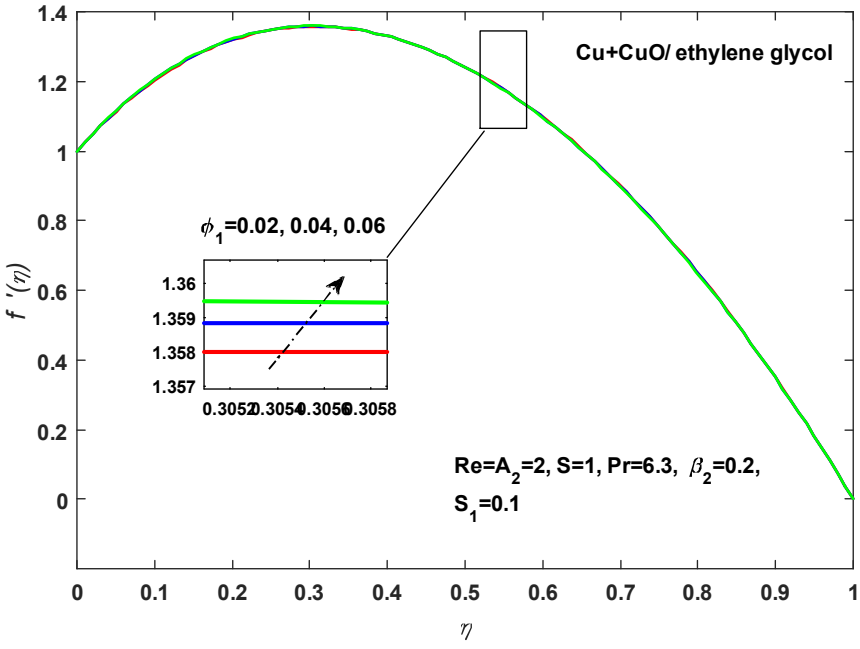

Fig. 4.2(b) Change in f′ (η) vs. ϕ

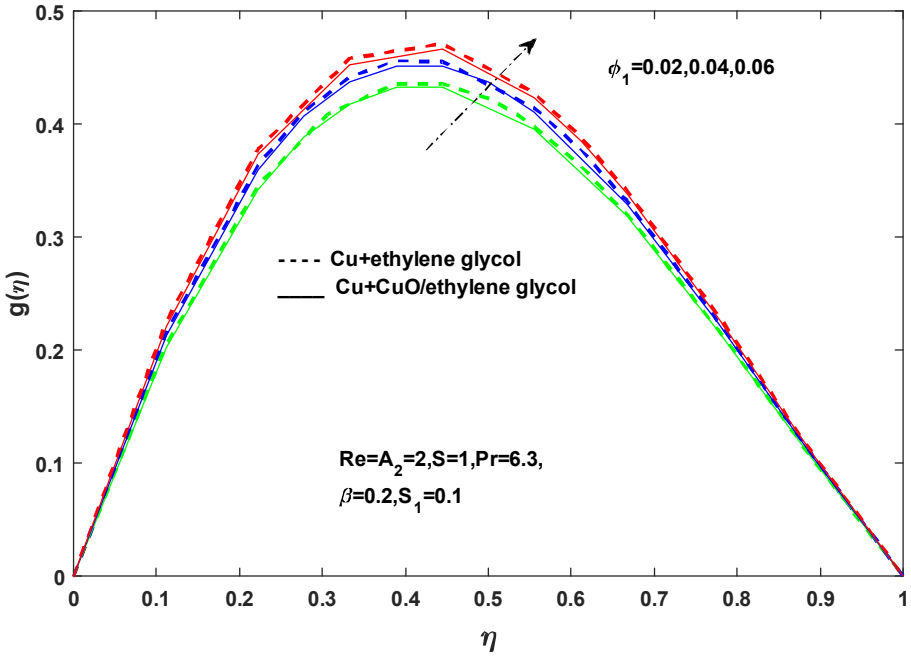

Fig. 4.3 Change in g(η) vs. ϕ

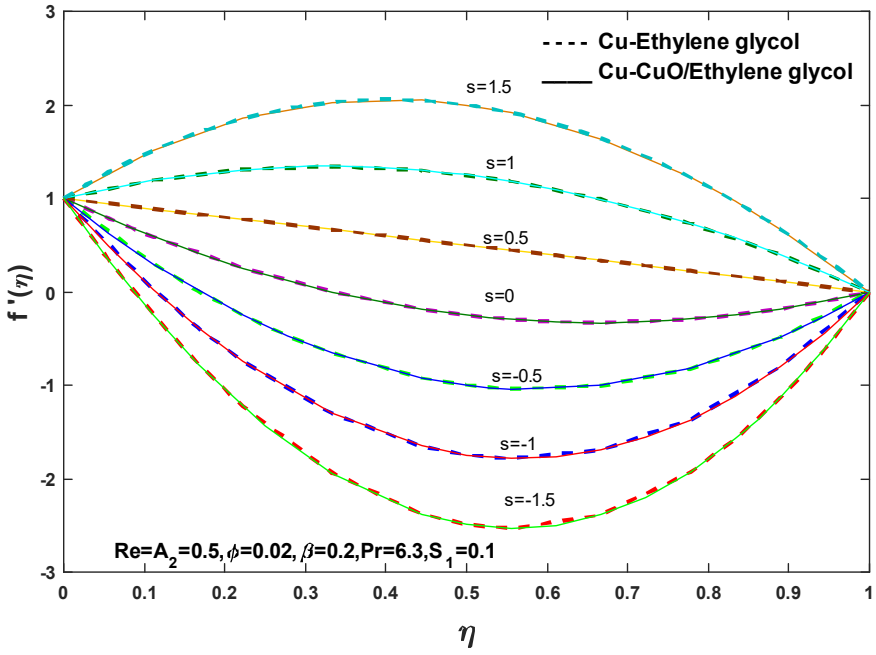

Fig. 4.4 Change in f′ (η) vs. S

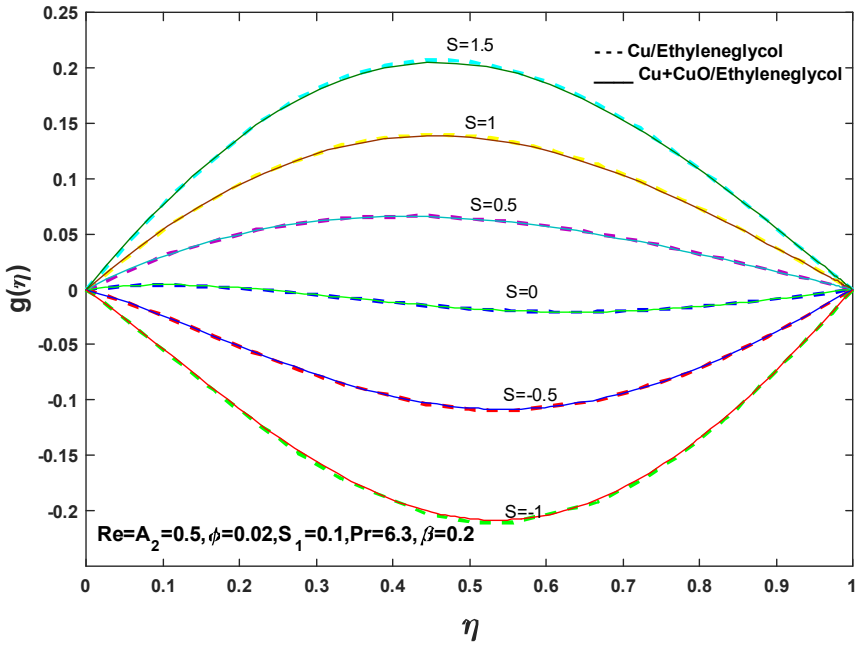

Fig. 4.5 Change in g(η) vs. S

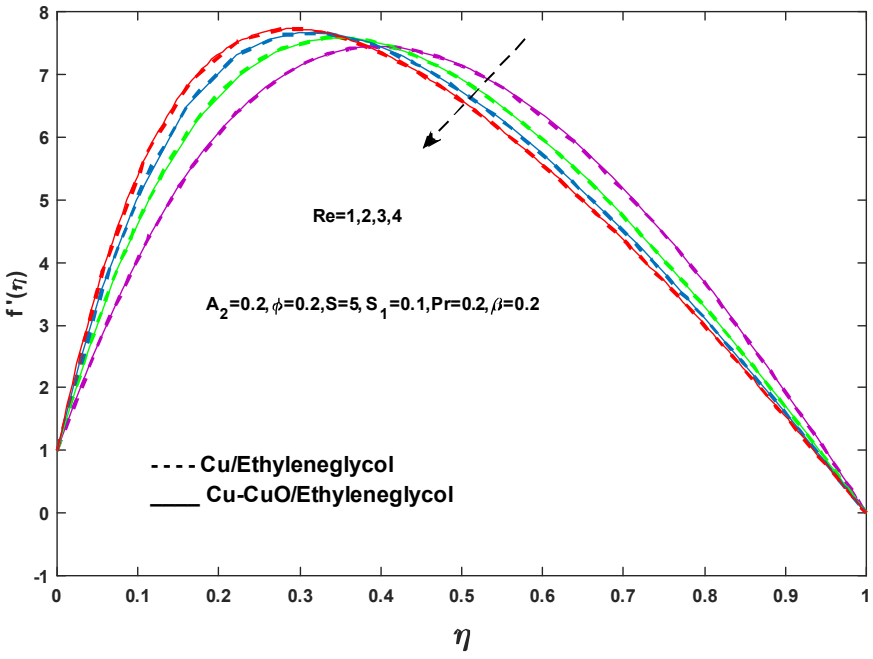

Fig. 4.6 Change in f′ (η) vs. Re

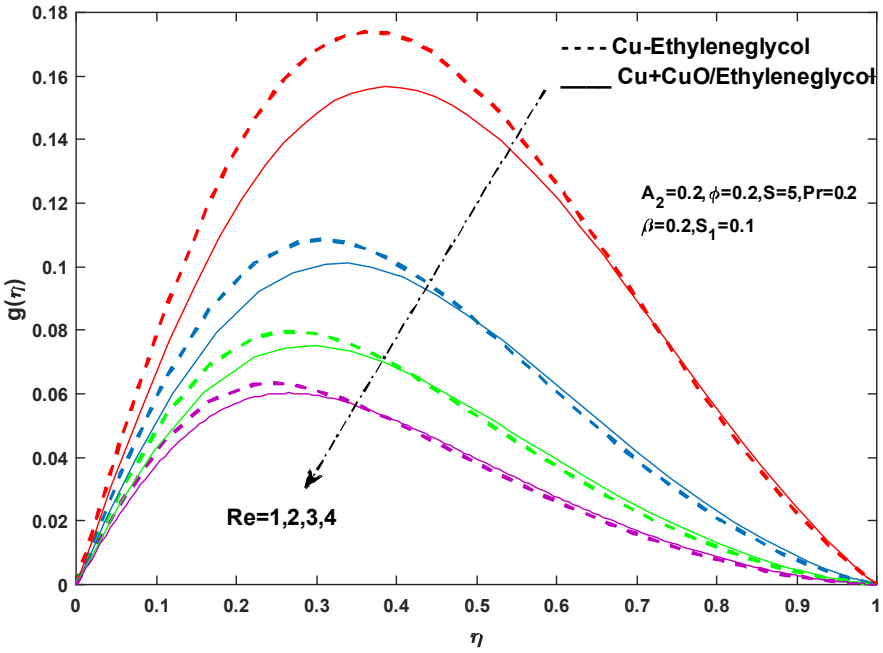

Fig. 4.7 Change in g(η) vs. Re

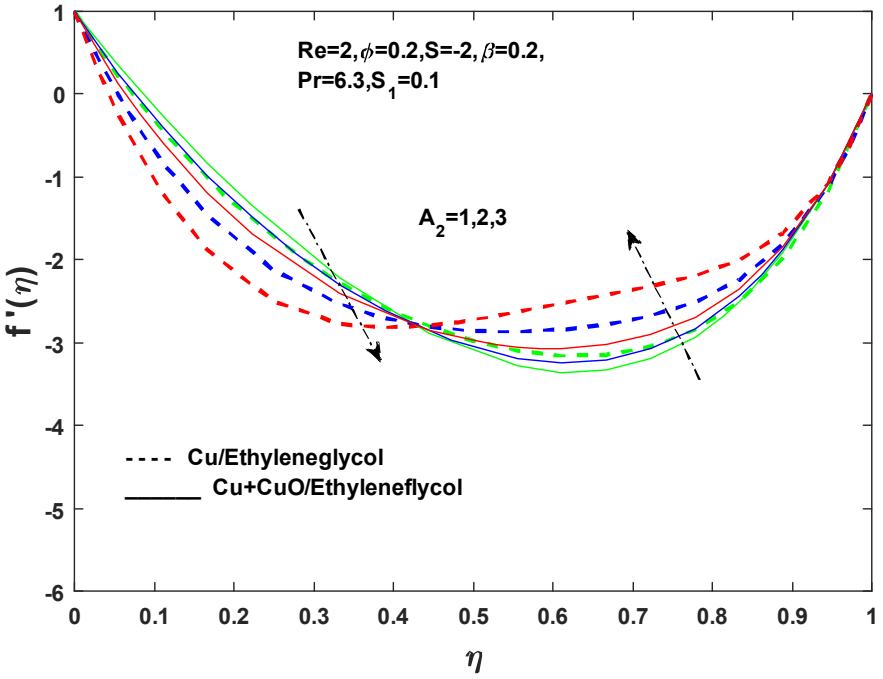

Fig. 4.8 Change in f′ (η) vs. A_2

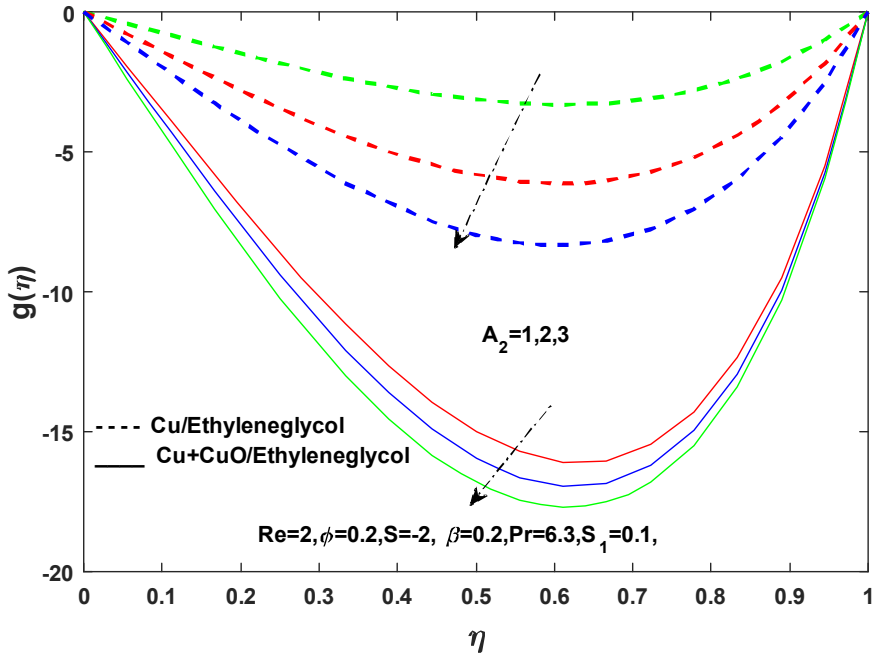

Fig. 4.9 Change in g(η) vs. A_2

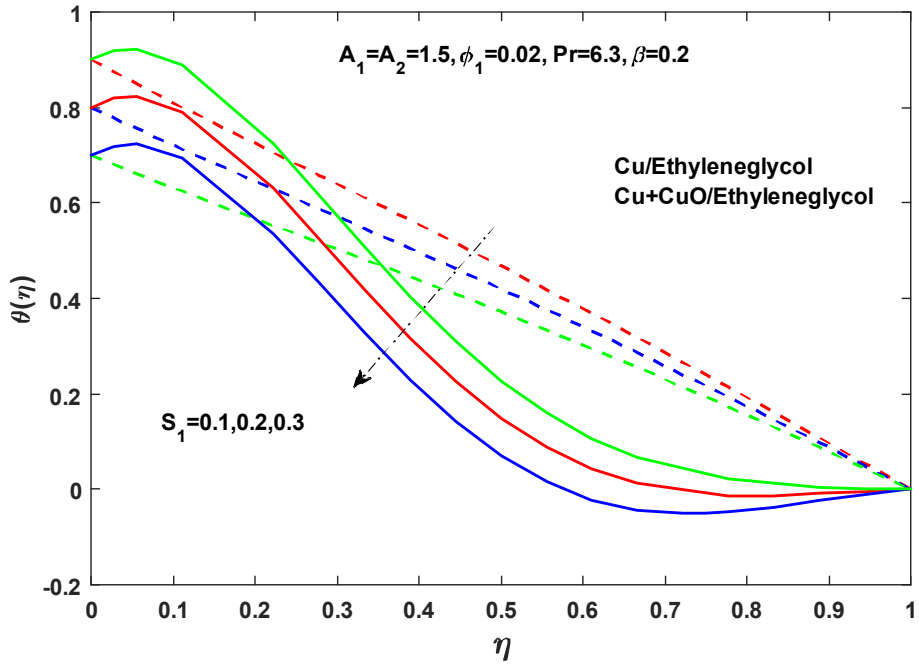

Fig. 4.10 Change in $\theta(\eta)$ vs. S_1

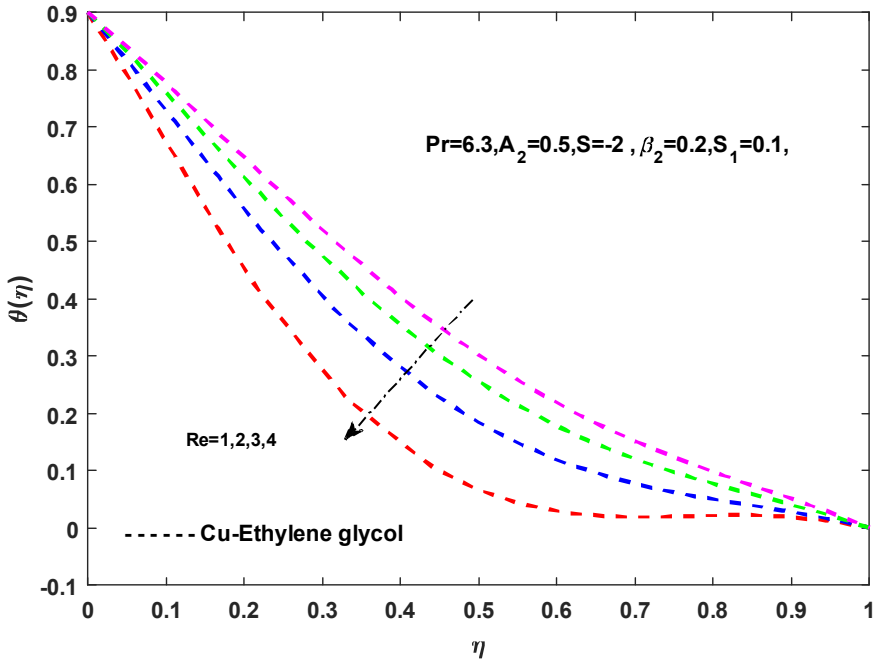

Fig. 4.11(a) Change in $\theta(\eta)$ vs. Re

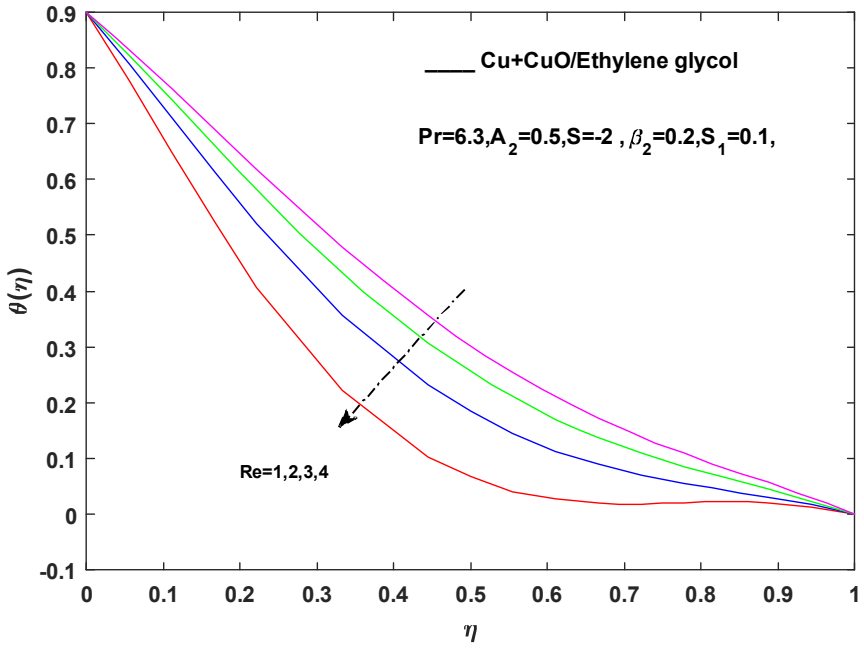

Fig. 4.11(b) Change in $\theta(\eta)$ vs. Re

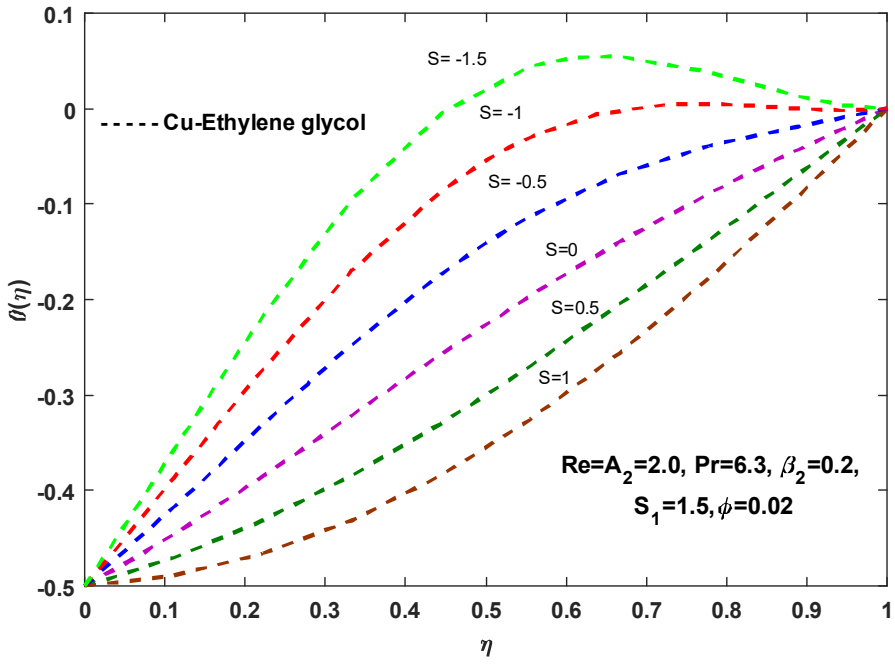

Fig. 4.12(a) Change in $\theta(\eta)$ vs. S

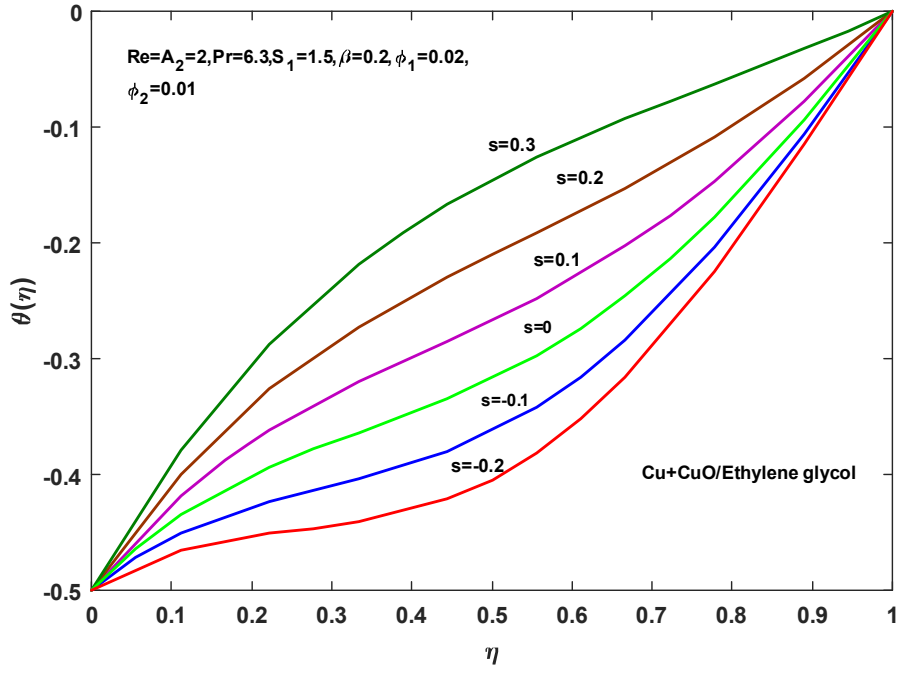

Fig. 4.12(b) Change in $\theta(\eta)$ vs. S

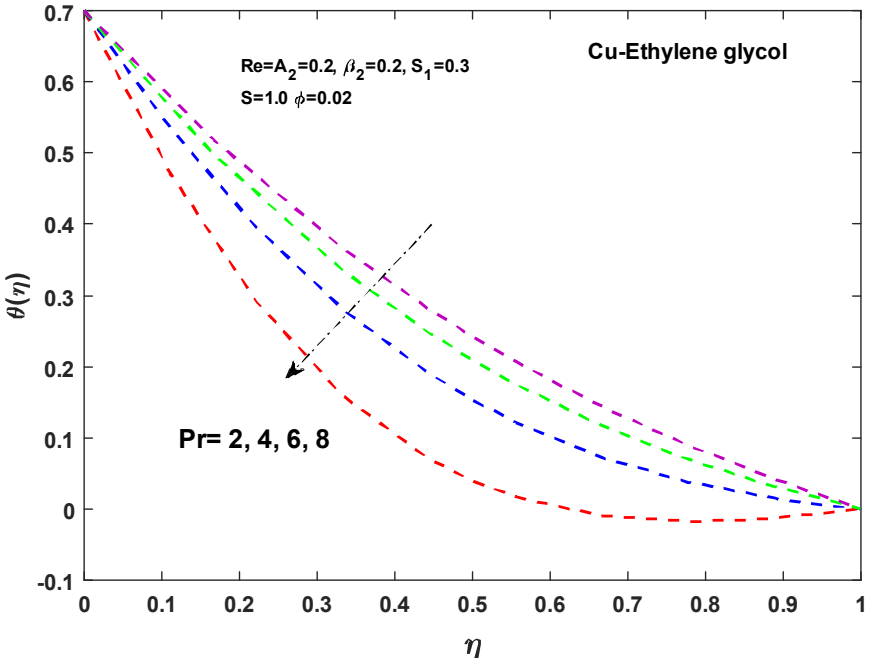

Fig. 4.13(a) Change in $\theta(\eta)$ vs. Pr

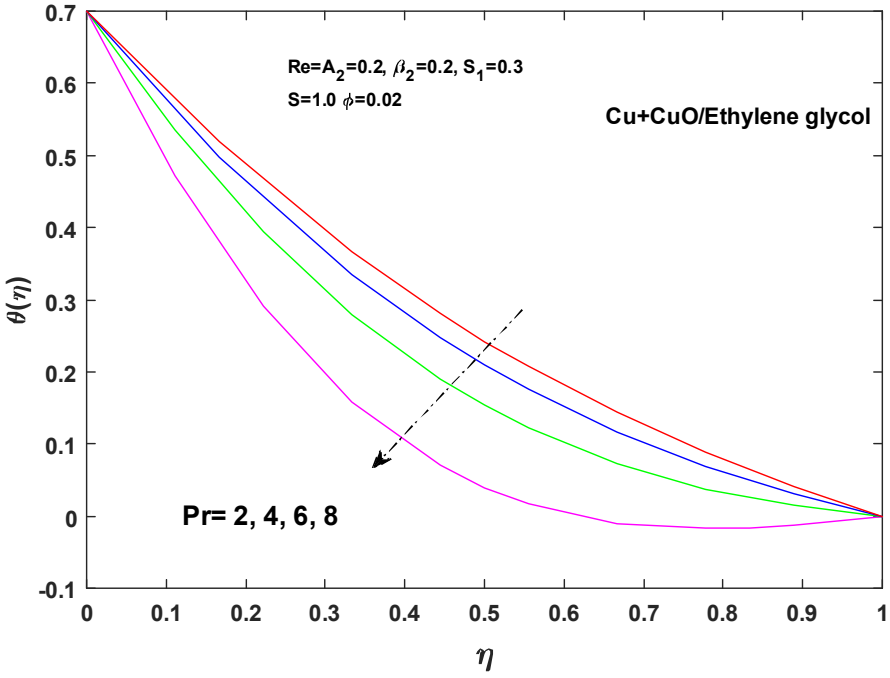

Fig. 4.13(b) Change in $\theta(\eta)$ vs. Pr

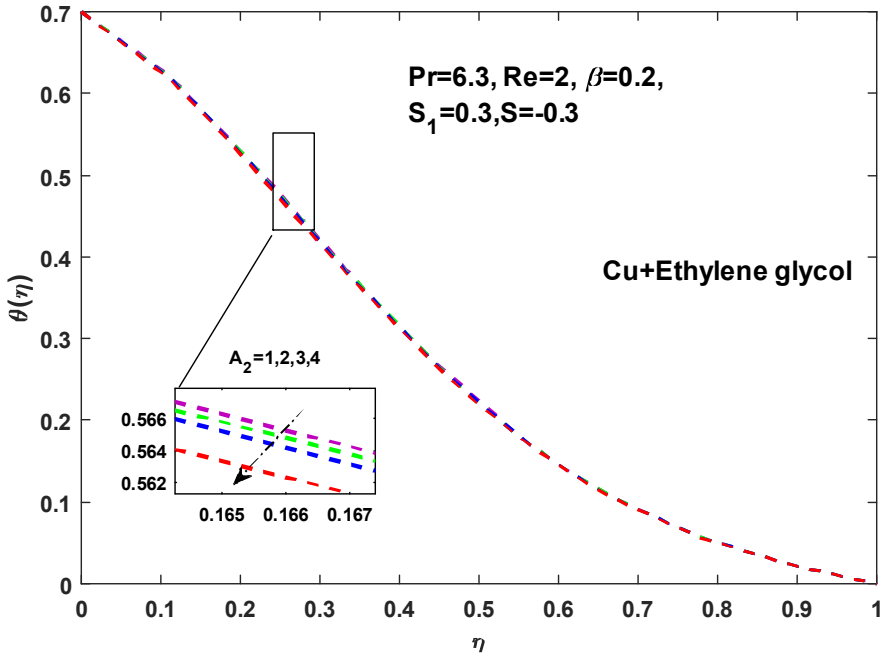

Fig. 4.14(a) Change in $\theta(\eta)$ vs. A_2

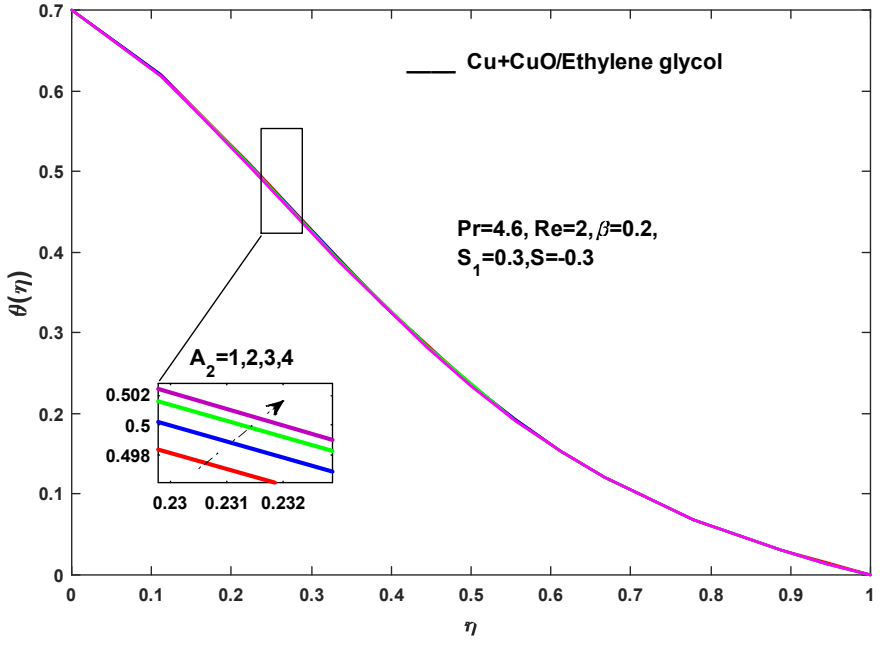

Fig. 4.14(b) Change in $\theta(\eta)$ vs. A_2

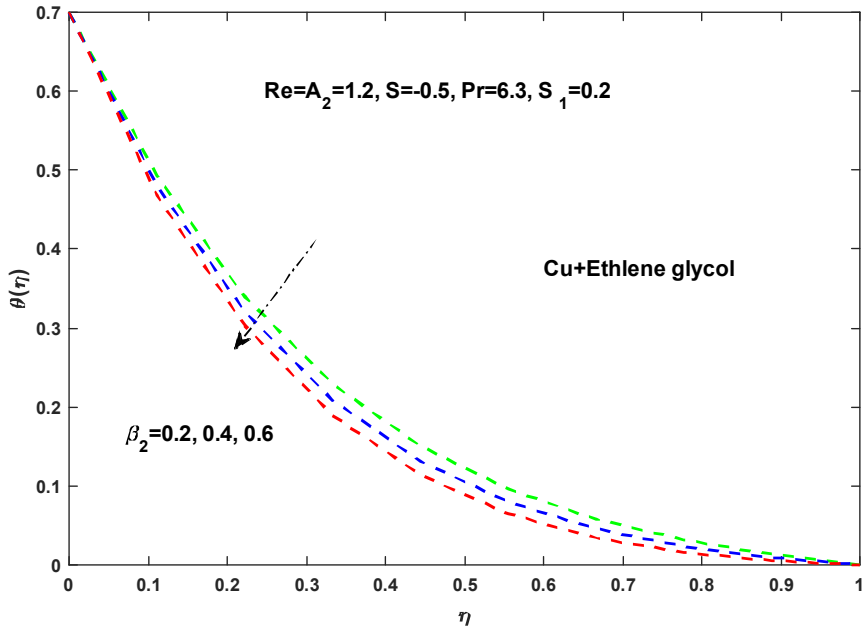

Fig. 4.15(a) Change in $\theta(\eta)$ vs. β_2

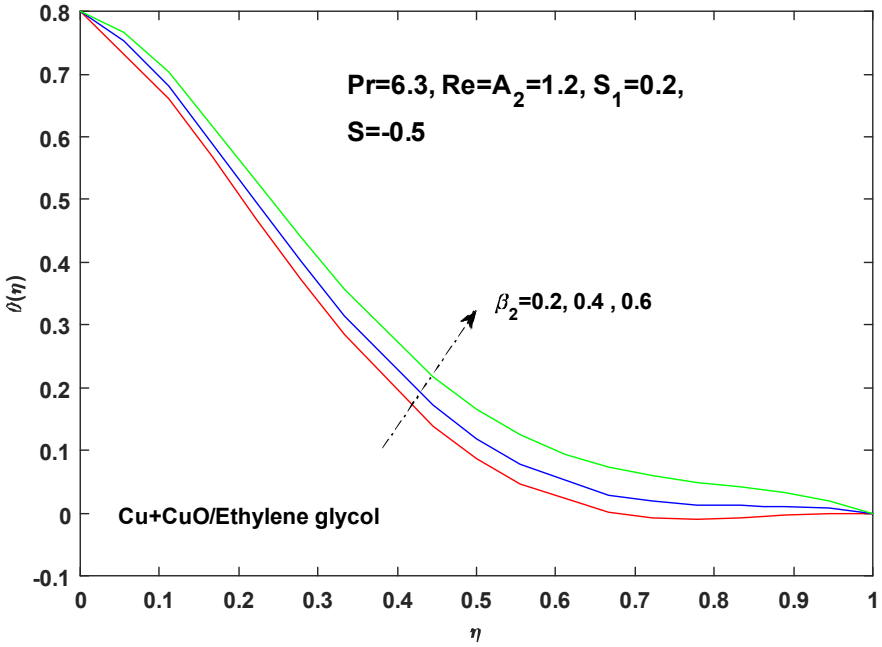

Fig. 4.15(b) Change in $\theta(\eta)$ vs. β_2

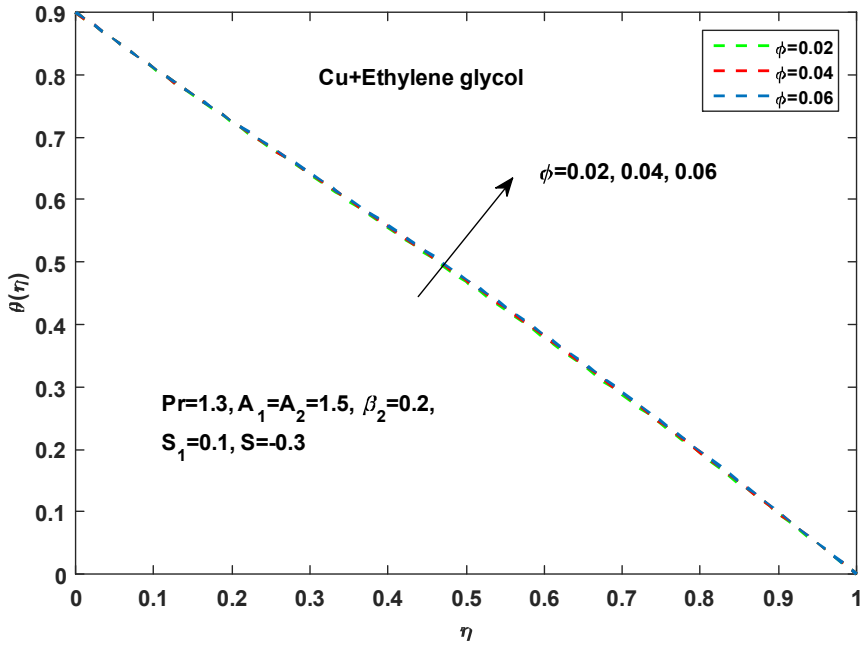

Fig. 4.16(a) Change in $\theta(\eta)$ vs. ϕ

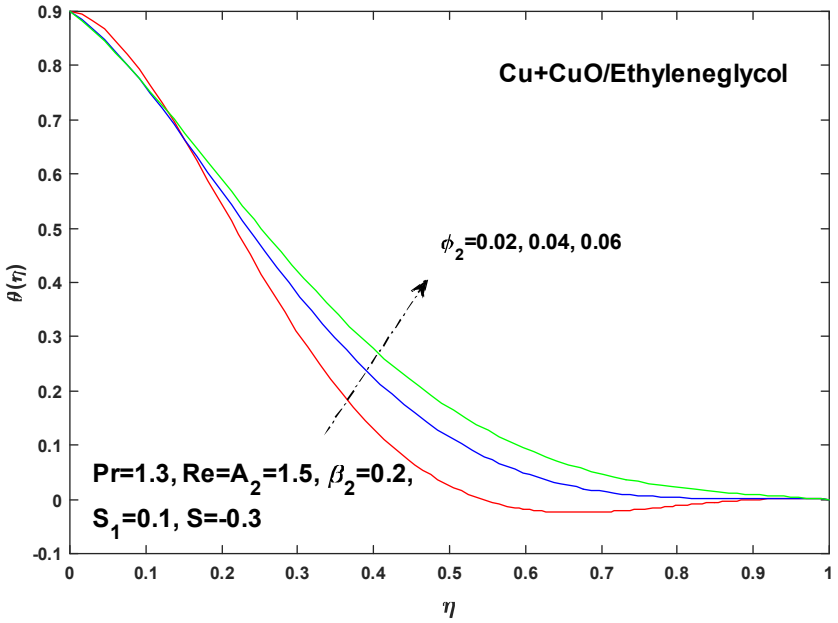

Fig. 4.16(b) Change in $\theta(\eta)$ vs. ϕ

Chapter 5

Conclusions and future work

In this thesis the first problem is review work and second problem is the extension work. The following are the conclusions of both problems :-

5.1 Chapter 3

The significant features of this problem is mentioned below:

- For nanoparticle volume fraction ϕ, an opposite trend is analyzed against two velocities $f'(\eta),\ g(\eta)$ in SWCNTs and MWCNTs.
- For suction/injection, strength of velocity field increases.
- The temperature of fluid is decreases as thermal stratification parameter S_1 is augmented.
- For mounting values of nanoparticle volume fraction ϕ, and suction/injection parameter, drag force coefficient depicts opposite behavior at upper and lower plate for both CNTs (SWCNTs and MWCNTs).

5.2 Chapter 4

The following conclusions of this problem is mentioned below :-

- An augmentation in thermal stratification parameter,shows reduction in dimensionless temperature $\theta(\eta)$.
- Rotation parameter has an opposite behavior on both velocities $f'(\eta)$, $g(\eta)$and the temperature profile $\theta(\eta)$.
- Prandtl number shows decreasing trend against temperature on hybrid nanofluid .
- For suction/injection parameter, velocities and temperature profile shows an increasing behavior for mounting values of S, and reduction for small values of S in case of hybrid nanofluid.
- Reynolds number shows reduction for hybrid nanofluid for temperature profile.
- Thermal relaxation parameter shows decreasing behavior for both nanofluid and hybrid nanofluid against temperature profile.
- Drag force coefficient shows reduction at lower wall while enhancement at upper wall for escalating values of nanoparticle volume fraction and suction / injection parameter.

5.3 Future work

In this work the effects of non linear thermal stratification with modified Fourier's law on hybrid nanofluid have been analyzed. However, there is still space to design on existing work in order to improve concern discourse. Few interesting possible extensions that could be researched in future are as follows:-

- Any other non Newtonian fluid with suitable boundary conditions.

- Bio-convective nanofluid along with microorganisms.
- Flow over a curved surface with activation energy.
- Boundary conditions can be changed to melting heat.

Bibliography

[1] Eastman, J. A., Choi, S. U. S., Li, S., Yu, W., & Thompson, L. J. (2001). Anomalously increased effective thermal conductivities of ethylene glycol-based nanofluids containing copper nanoparticles. Applied physics letters, 78(6), 718-720.

[2] Turcu, R., Darabont, A. L., Nan, A., Aldea, N., Macovei, D., Bica, D., ... & Biro, L. P. (2006). New polypyrrole-multiwall carbon nanotubes hybrid materials. Journal of optoelectronics and advanced materials, 8(2), 643-647.

[3] Esfe, M. H., Wong wises, S., Naderi, A., Asadi, A., Safaei, M. R., Rostamian H., (2015). Thermal conductivity of Cu/TiO_2-water/ EG hybrid nanofluid International communication Heat Mass Transfer 66, 100-104.

[4] Esfe, M. H., Arani, A. A. A., Rezaie, M., Yan, W. M., & Karimipour, A. (2015). Experimental determination of thermal conductivity and dynamic viscosity of Ag–MgO/water hybrid nanofluid. International Communications in Heat and Mass Transfer, 66, 189-195.

[5] Esfe, M. H., Yan, W. M., Akbari, M., Karimipour, A., & Hassani, M. (2015). Experimental study on thermal conductivity of DWCNT-ZnO/water-EG nanofluids. International Communications in Heat and Mass Transfer, 68, 248-251..

[6] Mukhopadhyay, S., & Ishak, A. (2012). Mixed convection flow along a stretching cylinder in a thermally stratified medium. Journal of Applied Mathematics, 2012.

[7] Ibrahim, W., & Makinde, O. D. (2013). The effect of double stratification on boundary-layer flow and heat transfer of nanofluid over a vertical plate. Computers & Fluids, 86, 433-441.

[8] baron Fourier, J. B. J. (1822). Théorie analytique de la chaleur. Chez Firmin Didot, père et fils.

[9] Narasimhan, T. N., (1999) , Fourier's Heat Conduction equation", Reviews of Geophysics 37(1), 151-172.

[10] Cattaneo, C. (1948). Sulla conduzione del calore. Atti Sem. Mat. Fis. Univ. Modena, 3, 83-101.

[11] Christov, C. I. (2009). On frame indifferent formulation of the Maxwell–Cattaneo model of finite-speed heat conduction. Mechanics Research Communications, 36(4), 481-486.

[12] Khan, S. K., & Sanjayanand, E. (2005). Viscoelastic boundary layer flow and heat transfer over an exponential stretching sheet. International Journal of Heat and Mass Transfer, 48(8), 1534-1542.

[13] Rubab, K., & Mustafa, M. (2016). Cattaneo-Christov heat flux model for MHD three-dimensional flow of Maxwell fluid over a stretching sheet. PLoS One, 11(4), e0153481.

[14] Tibullo, V., & Zampoli, V. (2011). A uniqueness result for the Cattaneo–Christov heat conduction model applied to incompressible fluids. Mechanics Research Communications, 38(1), 77-79.

[15] Choi, S. U., & Eastman, J. A. (1995). Enhancing thermal conductivity of fluids with nanoparticles (No. ANL/MSD/CP-84938; CONF-951135-29). Argonne National Lab., IL (United States).

[16] Mi, G., Shi, D., Wang, M., & Webster, T. J. (2018). Reducing bacterial infections and biofilm formation using nanoparticles and nanostructured antibacterial surfaces. Advanced Healthcare Materials, 7(13), 1800103..

[17] Sheikholeslami, M., Hayat, T., & Alsaedi, A. (2017). RETRACTED: Numerical simulation of nanofluid forced convection heat transfer improvement in existence of magnetic field using lattice Boltzmann method..

[18] Ramzan, M., Sheikholeslami, M., Saeed, M., & Chung, J. D. (2019). On the convective heat and zero nanoparticle mass flux conditions in the flow of 3D MHD Couple Stress nanofluid over an exponentially stretched surface. Scientific reports, 9(1), 1-13.

[19] Murshed, S. S., De Castro, C. N., Lourenço, M. J. V., Lopes, M. L. M., & Santos, F. J. V. (2011). A review of boiling and convective heat transfer with nanofluids. Renewable and Sustainable Energy Reviews, 15(5), 2342-2354.

[20] Sarkar, J., Ghosh, P., & Adil, A. (2015). A review on hybrid nanofluids: recent research, development and applications. Renewable and Sustainable Energy Reviews, 43, 164-177.

[21] Hayat, T., & Nadeem, S. (2017). Heat transfer enhancement with Ag–CuO/water hybrid nanofluid. Results in physics, 7, 2317-2324.

[22] Tiwari, R. K., & Das, M. K. (2007). Heat transfer augmentation in a two-sided lid-driven differentially heated square cavity utilizing nanofluids. International Journal of heat and Mass transfer, 50(9-10), 2002-2018..

[23] Devi, S. A., & Devi, S. S. U. (2016). Numerical investigation of hydromagnetic hybrid Cu–Al2O3/water nanofluid flow over a permeable stretching sheet with suction. International Journal of Nonlinear Sciences and Numerical Simulation, 17(5), 249-257.

[24] Khashi'ie, N. S., Arifin, N. M., Pop, I., & Wahid, N. S. (2020). Flow and heat transfer of hybrid nanofluid over a permeable shrinking cylinder with Joule heating: a comparative analysis. Alexandria Engineering Journal, 59(3), 1787-1798.

[25] Malvandi, A., Hedayati, F., & Nobari, M. R. H. (2014). An HAM analysis of stagnation-point flow of a nanofluid over a porous stretching sheet with heat generation. Journal of Applied Fluid Mechanics, 7(1), 135-145.

[26] Tsai, R., Huang, K. H., & Huang, J. S. (2008). Flow and heat transfer over an unsteady stretching surface with non-uniform heat source. International Communications in Heat and Mass Transfer, 35(10), 1340-1343..

[27] Hayat, T., Ijaz Khan, M., Shehzad, S. A., Imran Khan, M., & Alsaedi, A. (2018). Numerical simulation of Darcy–Forchheimer flow of third grade liquid with Cattaneo–Christov heat flux model. Mathematical Methods in the Applied Sciences, 41(12), 4352-4359.

[28] Lu, D., Li, Z., Ramzan, M., Shafee, A., & Chung, J. D. (2019). Unsteady squeezing carbon nanotubes based nano-liquid flow with Cattaneo–Christov heat flux and homogeneous–heterogeneous reactions. Applied Nanoscience, 9(2), 169-178.

[29] Alamri, S. Z., Khan, A. A., Azeez, M., & Ellahi, R. (2019). Effects of mass transfer on MHD second grade fluid towards stretching cylinder: a novel perspective of Cattaneo–Christov heat flux model. Physics Letters A, 383(2-3), 276-281.

[30] Ramzan, M., Gul, H., & Sheikholeslami, M. (2019). Effect of second order slip condition on the flow of tangent hyperbolic fluid—A novel perception of Cattaneo–Christov heat flux. Physica Scripta, 94(11), 115707..

[31] Ali, U., Alqahtani, A. S., Rehman, K. U., & Malik, M. Y. (2019). On Cattaneo-Christov heat flux analysis with magneto-hydrodynamic and heat generation effects in a Carreau nano-fluid over a stretching sheet. Revista mexicana de física, 65(5), 479-488..

[32] Ramzan, M., & Shaheen, N. (2019). Thermally stratified Darcy–Forchheimer nanofluid flow comprising carbon nanotubes with effects of Cattaneo–Christov heat flux and homogeneous–heterogeneous reactions. Physica Scripta, 95(1), 015701.

[33] Goodman, S. (1957). Radiant-heat transfer between non gray parallel plates. Journal of Research of the National Bureau of Standards, 58(1), 37-40.

[34] Sheikholeslami, M., Rashidi, M. M., Al Saad, D. M., Firouzi, F., Rokni, H. B., & Domairry, G. (2016). Steady nanofluid flow between parallel plates considering thermophoresis and Brownian effects. Journal of King Saud University-Science, 28(4), 380-389.

[35] Ahmed, N., Mohyud-Din, S. T., & Hassan, S. M. (2016). Flow and heat transfer of nanofluid in an asymmetric channel with expanding and contracting walls suspended by carbon nanotubes: a numerical investigation. Aerospace Science and Technology, 48, 53-60.

[36] Vajravelu, K., & Kumar, B. V. R. (2004). Analytical and numerical solutions of a coupled non-linear system arising in a three-dimensional rotating flow. International Journal of Non-Linear Mechanics, 39(1), 13-24.

[37] Hayat, T., Muhammad, K., Farooq, M., & Alsaedi, A. (2016). Squeezed flow subject to Cattaneo–Christov heat flux and rotating frame. Journal of Molecular Liquids, 220, 216-222.

[38] Mehmood, A., & Ali, A. (2007). Analytic homotopy solution of generalized three-dimensional channel flow due to uniform stretching of the plate. Acta Mechanica Sinica, 23(5), 503-510..

[39] Mehmood, A., & Ali, A. (2011). Across mass transfer phenomenon in a channel of lower stretching wall. Chemical Engineering Communications, 198(5), 678-691.

[40] Hussain, S., Mehmood, A., Ali, A. (2014). Three diemensional channel flow of second grade fluid in a rotating frame Applied Mathematics and Mechanics 35(7), 777-789.

[41] Lu, D., Ramzan, M., Ahmad, S., Shafee, A., & Suleman, M. (2018). Impact of non-linear thermal radiation and entropy optimization coatings with hybrid nanoliquid flow past a curved stretched surface. Coatings, 8(12), 430.

[42] Iqbal, Z., Akbar, N. S., Azhar, E., & Maraj, E. N. (2018). Performance of hybrid nanofluid (Cu-CuO/water) on MHD rotating transport in oscillating vertical channel inspired by Hall current and thermal radiation. Alexandria engineering journal, 57(3), 1943-1954.

[43] Sheikholeslami, M., Rashidi, M. M., Al Saad, D. M., Firouzi, F., Rokni, H. B., & Domairry, G. (2016). Steady nanofluid flow between parallel plates considering thermophoresis and Brownian effects. Journal of King Saud University-Science, 28(4), 380-389.

[44] Eldabe, N. T., Elsaka, A. G., Radwan, A. E., & Eltaweel, M. A. (2010). Effects of chemical reaction and heat radiation on the MHD flow of viscoelastic fluid through a porous medium over a horizontal stretching flat plate. J. Am. Sci, 6(9), 126-136.

[45] Hayat, T., & Nadeem, S. (2017). Heat transfer enhancement with Ag–CuO/water hybrid nanofluid. Results in physics, 7, 2317-2324.

[46] M.Meznar, (2005). Fluid Flows in a Rotating frame.

[47] Pak, B. C.& Cho, Y. I. (1998). Hydrodynamic and heat transfer study of dispersed fluids with submicron metallic oxide particles. Experimental Heat Transfer an International Journal, 11(2), 151-170.

[48] Brinkman, H. C., (1952) .The viscosity of concentrated suspensions and solutions, The Journal of Chemical Physics, 20(4), 571,

[49] Xue, Q. Z., (2005). Model for thermal conductivity of carbon nanotube-based composites. Physica B: Condensed Matter, 368(1), 302–307.

[50] Babu, J. R., Kumar, K. K., & Rao, S. S. (2017). State-of-art review on hybrid nanofluids. Renewable and Sustainable Energy Reviews, 77, 551-565.

[51] Alosious, S., Sarath, S. R., Nair, A. R., & Krishnakumar, K. (2018). Investigations on Convective Heat Transfer Enhancement in Circular Tube Radiator Using Al2O3 and CuO Nanofluids. Journal of Thermal Science and Engineering Applications, 10(5)..

[52] Kandasamy, R., & Muhammad, R. (2016). Thermal radiation energy on squeezed MHD flow of Cu, Al2O3 and CNTs-nanofluid over a sensor surface. Alexandria Engineering Journal, 55(3), 2405-2421..

Noor e Saba

ORIGINALITY REPORT

2%	2%	1%	%
SIMILARITY INDEX	INTERNET SOURCES	PUBLICATIONS	STUDENT PAPERS

PRIMARY SOURCES

1	www.cambridge.org Internet Source	1%
2	darwin.bth.rwth-aachen.de Internet Source	1%
3	docsplayer.net Internet Source	<1%

Exclude quotes	On	Exclude matches	< 5 words
Exclude bibliography	On		